Delay Analysis of Max-Weight Queue Algorithm for Time-varying Wireless Adhoc Networks - Control Theoretical Approach

Junting Chen, *Student Member, IEEE* and Vincent K. N. Lau, *Fellow, IEEE*

Dept. of Electronic and Computer Engineering

The Hong Kong University of Science and Technology

Clear Water Bay, Kowloon, Hong Kong

Email: {eejtchen, eeknlau}@ust.hk

Abstract

Max weighted queue (MWQ) control policy is a widely used cross-layer control policy that achieves queue stability and a reasonable delay performance. In most of the existing literature, it is assumed that optimal MWQ policy can be obtained instantaneously at every time slot. However, this assumption may be unrealistic in time varying wireless systems, especially when there is no closed-form MWQ solution and iterative algorithms have to be applied to obtain the optimal solution. This paper investigates the convergence behavior and the queue delay performance of the conventional MWQ iterations in which the channel state information (CSI) and queue state information (QSI) are changing in a similar timescale as the algorithm iterations. Our results are established by studying the stochastic stability of an equivalent virtual stochastic dynamic system (VSDS), and an extended Foster-Lyapunov criteria is applied for the stability analysis. We derive a closed form delay bound of the wireless network in terms of the CSI fading rate and the sensitivity of MWQ policy over CSI and QSI. Based on the equivalent VSDS, we propose a novel MWQ iterative algorithm with compensation to improve the tracking performance. We demonstrate that under some mild conditions, the proposed modified MWQ algorithm converges to the optimal MWQ control despite the time-varying CSI and QSI.

Index Terms

Max Weighted Queue, Convergence Analysis, Queue Stability, Forster-Lyapunov, Stochastic Stability

I. INTRODUCTION

Recently, there has been intense research interest studying cross-layer resource allocation of wireless adhoc networks for delay-sensitive applications. While the CSI indicates the *transmission opportunity*, the *queue-state-information* indicates the *urgency* of the packets in the queues. A good control policy (in delay sense) should strike a balance between the opportunity (CSI) and the urgency (QSI) and the design is highly non-trivial [1]–[6]. One approach, namely the *Lyapunov Optimization* technique [5], [6], allows a potentially simple control policy which adapts to the CSI and QSI. Specifically, the authors in [5], [6] have proven that a *max weighted queue* (MWQ) throughput optimization solution can maximize the negative Lyapunov drift in the queue dynamics and it can achieve queue stability[1] with reasonable delay performance.

In most of the existing literature, it has been commonly assumed that the MWQ policy can be solved efficiently at each time slot based on the current realizations of CSI and QSI. However, this assumption may not be practical for moderate to large scale networks. Specifically, the MWQ solution requires solving a queue-weighted optimization problem [5], [6] and there is no closed-form solution in most cases. As a result, iterative algorithms (such as primal dual iterations) have to be used to obtain the MWQ solution at each time slot. While there is a lot of standard literature establishing the convergence of the iterative optimization algorithms, these works have assumed that the CSI and the QSI remains unchanged during the algorithm iterations[2]. However, for large scale networks, the algorithm iteration may involve not only the node itself but also over-the-air signaling between nodes. In this case, the CSI and the QSI may have changed after a few iterations and the existing convergence results (for static problems) failed to apply in this case of time-varying CSI and QSI. Furthermore, when the nodes in the adhoc network have limited power and computational resources, it may not be cost-effective for the node to iterate many times locally at each time slot as well. These observations motivate us to study the design and delay analysis of MWQ solutions in time varying wireless adhoc networks.

In this paper, we consider a time-varying wireless adhoc network with power control driven by the MWQ algorithm. We study how the average delay performance of the MWQ solution is affected by the time-varying CSI and QSI. Unlike conventional works, we focus on the case where the MWQ algorithm iteration evolves in a similar timescale as the CSI and QSI dynamics. There are various first order technical challenges that have to be addressed.

- **Nonlinear Stochastic Algorithm Dynamics:** One approach is to adopt continuous time con-

---

[1]Using the MWQ solution, the system of queues can be stable if the arrival rates are within the *stability region* [5] of the systems.

[2]In other words, it is assumed that the algorithm iteration time scale is much smaller than the CSI / QSI time scale.

trol theory and model the algorithm dynamics using deterministic ODE [7]–[11]. In [7]–[9], the authors have considered the convergence behavior of the Foschini-Miljanic power control algorithm under time varying channels using the linear ordinary differential equation (ODE) approach. The authors in [10], [11] studied the tracking performance of the linear least mean square (LMS) algorithms under time varying channels. However, all these works have assumed *linear and deterministic* algorithm dynamics and these approaches cannot be easily extended to our case where the MWQ algorithm iteration is *nonlinear and stochastic*.

- **Coupled Queue Dynamics and Algorithm Dynamics:** The evolution of QSI depends on the control actions of the MWQ algorithm in each time slot. On the other hand, the evolution of the MWQ algorithm also depends on the time-varying QSI because the MWQ solution is obtained by solving a queue-weighted optimization. As a result of this mutual coupling, the techniques in our previous works [12], which considered algorithm tracking performance where control decisions were made only based on CSI, cannot be easily extended in this case[3].

- **Delay Analysis and Compensation with Algorithm Tracking Errors:** It is also quite challenging to analyze and compensate for the delay penalty due to the MWQ algorithm tracking errors on the power control actions. In [5], [6], the authors have derived an average delay bound for MWQ algorithm with i.i.d. CSI based on the Lyapunov drift analysis. However, this technique cannot be easily extended to our case when there are tracking errors in the MWQ control actions and correlations in the CSI evolutions.

In this paper, we adopt a continuous time approach to model the algorithm dynamics of the MWQ power control iterations. We consider Markovian source arrivals and CSI evolutions so that the combined CSI, QSI and algorithm dynamics can be modeled by a *stochastic differential equation* (SDE). We show that studying the convergence behavior in the *algorithm domain* is equivalent to studying the *stability* property of a *virtual stochastic dynamic system* (VSDS). Using non-linear control theory and *stochastic Foster-Lyapunov* techniques, we establish a bound on delay performance due to time varying CSI and random source arrivals. Based on the VSDS dynamics, we propose a modification to the standard MWQ algorithm to compensate for the penalty due to the time-variation in the wireless adhoc networks. This paper provides a theoretical framework for studying the convergence of iterative algorithms as well as potential compensation techniques. The convergence analysis of iterative algorithms have widespread applications in network optimizations [3], [5], [6] and signal processing [10], [11].

---

[3]In the previous work [12], the control actions were made only based on the CSI. However, in this work, we consider CSI and QSI adaptive control policies and focus on the impact of *both* the time-varying CSI and QSI on the convergence of the algorithm. Here, there is a coupled dependency between the control actions (which depends on QSI) and the time-varying QSI (which depends on the control actions). This coupled dependency makes the problem challenging.
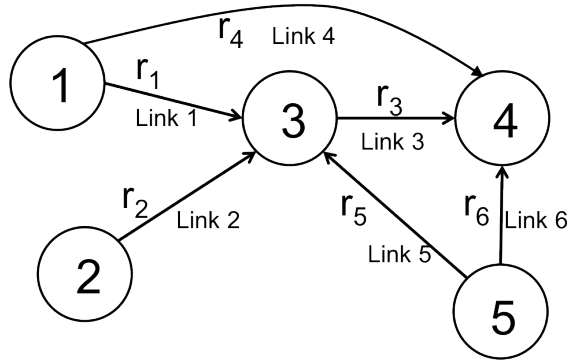
Figure 1. Network topology. We consider a wireless adhoc network with N nodes and L links. We illustrate here $N = 5$ and $L = 6$ as an example. The l-th link transmits the l-th data flow. Transmission flows towards a same destination share the same frequency band and MUD and SIC are implemented at each receiving node to handle the inter-flow interference.

Notations: A^T ($\mathbf{a}^T$) denotes the transpose of matrix (vector) A ($\mathbf{a}$) and A^H denotes the complex conjugate transpose. $|x|$ denotes the absolute value of x and $\|\mathbf{x}\| = \max_i\{x_i\}$ denotes the L_∞ norm of vector $\mathbf{x}$. For a complex variable z, $\text{Re}\,[z]$ denotes its real part and $\overline{z}$ denotes its complex conjugate.

II. SYSTEM MODEL AND VIRTUAL STOCHASTIC DYNAMIC SYSTEMS

In this section, we shall first introduce the system model of the wireless adhoc network as well as the MWQ algorithm. Next, we shall introduce the notion of *virtual stochastic dynamic system* and establish the equivalence between the convergence behavior of the gradient algorithm and the *virtual stochastic dynamic system*.

A. Network Topology, CSI and QSI Models

We consider a wireless adhoc network with N nodes and L links, where each link corresponds to one transmitting and receiving pair, as illustrated in Fig. 1. Different receiving nodes occupy different frequency bands, while transmission flows towards a same destination share the same frequency band. *Multiuser detection* (MUD) and *successive interference cancellation* (SIC) are implemented at each receiving node to handle the *inter-flow interference*. The maximum achievable transmission rate at receiving node n is a set of rates μ_l that satisfy the following conditions [13],

$$\sum_{l \in \mathcal{S}(n)} \mu_l < \log\left(1 + \sum_{l \in \mathcal{S}(n)} |h_l|^2 p_l\right) \qquad \forall \mathcal{S}(n) \subset \mathcal{L}_{rev}(n) \tag{1}$$

where $\mathcal{L}_{rev}(n)$ is a collection of links whose destinations are at node n, $\mathcal{S}(n)$ are any non-empty subsets of $\mathcal{L}_{rev}(n)$, h_l is the channel fading coefficients of link l and p_l is the normalized power allocated at link l. For example, Fig. 1 illustrates an example adhoc network with $N = 5$ nodes and

$L = 6$ links. $\mathcal{L}_{rev}(3) = \{1, 2, 5\}, \mathcal{L}_{rev}(4) = \{3, 4, 6\}$. Subscript l represents the link index as well as the flow index.

We have the following assumptions regarding the channel state (CSI) $h_l(t)$.

Assumption 1 (Temporally Correlated CSI Model): The support of the channel state process $h_l(t)$ is assumed to be $h_l \in \mathcal{H} = \{h \in \mathbb{C} : |h| \geq h_0\}$ for some positive h_0. Furthermore, $h_l(t)$ is a stochastic process described by the following reflective *stochastic differential equation* (SDE) in [14]

$$dh_l = -\frac{1}{2} a_l h_l dt + a_l^{\frac{1}{2}} dw_l + dv_l, \quad h_l \in \mathcal{H} \tag{2}$$

where a_l determines the temporal correlation of $h_l(t)$, $w_l(t)$ is the standard complex Wiener process with unit variance, and dv_l is the Skorohod reflection [14] term that satisfies $dv_l(t) \geq 0$ and $\int_0^\infty 1\{|h_l(t)| > h_0\} dv_l(t) = 0$. The fading process is independent w.r.t. the link index l. ∎

Note that $h_l(t)$ in (2) is a continuous time version of the auto-regressive (AR) process which has been widely used to model the dynamics of a correlated wireless fading channel [15]. It captures the CSI variation speed that affects the convergence behavior of the algorithm in a time-varying channel. It can be shown that the process $h_l(t)$ has a stationary distribution.

Incoming data packets randomly arrive at different nodes and are queued according to their destinations associated with particular transmission links. Let $q_l(t)$ and $N_l(t)$ be the current queue backlog of queue and the number of packets arrived, respectively, at the l-th queue at time t. We have the following assumptions regarding the bursty arrival process $N_l(t)$.

Assumption 2 (Bursty Source Model): The packet arrival $N_l(t)$ is a Poisson process with intensity λ_l. Specifically, $N_l(t)$ follows a probability law given by,

$$\Pr\left(N_l(t + dt) - N_l(t) = 1 \big| N_l(t)\right) = \lambda_l dt.$$

∎

The queueing dynamics of the wireless adhoc network can be described by the following SDE,

$$dq_l = -\mu_l dt + dN_l. \tag{3}$$

The first term in (3) corresponds to the packet departure and the second term corresponds to the random packet arrival. Using Little's Law [16], the average delay of the l-th link (l-th flow) is given by $\overline{T}_l = \overline{q}_l / \lambda_l$, where $\overline{q}_l$ is the average backlog for the l-th queue. As a result, there is no loss of generality to study the average queue length $\overline{q}_l$ as this is proportional to the average delay. Obviously, the average queue length (or average delay) of the wireless adhoc network depends on how we allocate the transmit power $p_l(t)$ and data rate $\mu_l(t)$ of each link in the network. In the next section, we shall briefly review the MWQ algorithm, which is known to be a *throughput optimal control* (in queue stability sense).

B. Queue Stability and Max-Weighted Queue (MWQ) Algorithm

There are different ways to control the power $p_l(t)$ and rates $\mu_l(t)$ of the wireless networks but a reasonable algorithm (in delay sense) should adapt to both the CSI (to capture good transmission opportunity) and the QSI (to capture the urgency). In particular, we are interested in control policy that achieves a maximum queue stability region. We now first define the notion of *queue stability*, *stability region* and *throughput optimal control*.

Definition 1 (Queueing Stability): A queue is called *stable* if $\limsup_{t\to\infty} \frac{1}{t} \int_0^t \mathbb{E}\left[\|\mathbf{q}(\tau)\|\right] < \infty$. ∎

The *stability region* $\overline{\mathcal{C}}$ is defined as the closure of the set of all the arrival rate vectors $\{\lambda_l\}$ that can be stabilized under some control algorithm that conforms to the power constraint $\mathbb{E}[\mathbf{p}] \in \mathcal{P}$ [5]. A control policy that is *throughput optimal* is characterized in the sense that it stabilizes all the arrival rate vectors $\{\lambda_l\}$ within the stability region $\overline{\mathcal{C}}$ [17]. The throughput optimal policy is not unique and there are various known methods to achieve the maximum queue stability region. For technical reasons, we define a convex compact domain $\mathcal{P} = \{p : 0 \le p \le 2^{L\lambda_{\max}}/h_0^2\}$. Using Lyapunov techniques, a *throughput optimal* (in stability sense) formulation for the power and rate control actions at each time slot t is given in the following.

Problem 1 (MWQ Formulation):

$$\max_{\mathbf{p}\in\mathcal{P},\boldsymbol{\mu}\succeq\mathbf{0}} \quad \sum_l \left[q_l(t)\mu_l(t) - Vp_l(t) \right] \tag{4}$$

$$\text{subject to} \quad \boldsymbol{\mu}(t) = (\mu_l(t),\ldots,\mu_l(t))^T \in \mathcal{C}(\mathbf{p}(t),\mathbf{h}(t)) \tag{5}$$

where the physical layer capacity region $\mathcal{C}(\mathbf{p}(t),\mathbf{h}(t))$ is a polyhedron defined by the constraints in (1) for all receiving nodes n. The parameter V acts as a Lagrange multiplier which controls the tradeoff between the average delay and the average power of the wireless network. ∎

Note that the MWQ optimization problem in (4)-(5) is parameterized by the current CSI $\mathbf{h}(t) = \{h_1(t),\ldots,h_L(t)\}$ and the QSI $\mathbf{q}(t) = \{q_1(t)\ldots q_L(t)\}$. As a result, the optimal solution $\mathbf{p}^*(\mathbf{h}(t),\mathbf{q}(t))$ and $\boldsymbol{\mu}^*(\mathbf{h}(t),\mathbf{q}(t))$ of the MWQ problem is also parameterized by the CSI and QSI $(\mathbf{h}(t),\mathbf{q}(t))$.

Due to the interference coupling in the MWQ problem, there are no closed form solutions for $\mathbf{p}^*(\mathbf{h},\mathbf{q})$ and $\boldsymbol{\mu}^*(\mathbf{h},\mathbf{q})$ despite the problem in (4)-(5) being convex. To solve the MWQ problem in (4)-(5), we first have the following lemma regarding the rate allocation $\hat{\boldsymbol{\mu}}(\mathbf{p};\mathbf{h},\mathbf{q})$ given the power.

Lemma 1 (Optimal rate allocation [18]): Let $\boldsymbol{\pi} = \{\pi(1),\pi(2),\ldots\pi(L)\}$ be a permutation of the flow indices sorted in descendent order of the QSI q_l, i.e. $q_{\pi(1)} \ge q_{\pi(2)} \ge \cdots \ge q_{\pi(L)}$. Given a power allocation $\mathbf{p} = [p_1,p_2,\ldots,p_L]$, the optimal rate allocation solution of the MWQ problem in (4)-(5)

is given by

$$\hat{\mu}_{\pi(1)} = \log\left(1 + \left|h_{\pi(1)}\right|^2 p_{\pi(1)}\right) \tag{6}$$

$$\hat{\mu}_{\pi(k)} = \log\left(1 + \sum_{i=1}^{k}\left|h_{\pi(i)}\right|^2 p_{\pi(i)}\right) - \log\left(1 + \sum_{i=1}^{k-1}\left|h_{\pi(i)}\right|^2 p_{\pi(i)}\right), \quad k = 2, \ldots, L \tag{7}$$

■

Intuitively, given a power allocation, the optimal rate allocation vector $\hat{\boldsymbol{\mu}} = \{\hat{\mu}_1, \ldots, \hat{\mu}_L\}$ is given by one of the vertices of the polyhedron $\mathcal{C}(\mathbf{p}, \mathbf{h})$. In addition, the vertices are achieved by the SIC with decoding order $\boldsymbol{\pi}$. As a result, finding the optimal $\hat{\boldsymbol{\mu}}(\mathbf{p}; \mathbf{h}, \mathbf{q})$ is equivalent to a linear programming problem, which requires L steps of iterations. Hence, we can focus on the power optimization in the MWQ problem given by

$$\max_{\mathbf{p}(t) \in \mathcal{P}} \quad \mathcal{L}(\mathbf{p}(t); \mathbf{h}(t), \mathbf{q}(t)) = \sum_{l=1}^{L} q_l(t)\hat{\mu}_l(\mathbf{p}(t); \mathbf{h}(t), \mathbf{q}(t)) - V\sum_{l=1}^{L} p_l(t). \tag{8}$$

Using an iterative projected gradient search algorithm to find the optimal solution in (8), we derive the following power control algorithms dynamics [19],

$$\dot{\mathbf{p}} = \kappa\left[\nabla\mathcal{L}\left(\mathbf{p}; \mathbf{h}(t), \mathbf{q}(t)\right)\right]_{\mathbf{p}}^{\mathcal{P}} \tag{9}$$

where κ is a step size parameter, and the entry-wide projection operator $[.]_z^{\mathcal{P}}$ is defined as $[x]_z^{\mathcal{P}} := 0$, if $z \in \partial\mathcal{P}$ is on the boundary of $\mathcal{P}$ and $z + x dt \in \mathcal{P}$, and $[x]_z^{\mathcal{P}} := x$, otherwise. Hence, the queue dynamics of the wireless adhoc network under MWQ control is determined by the following *coupled SDEs*.

$$dp_l = \kappa\left[\frac{\partial}{\partial p_l}\mathcal{L}\left(\mathbf{p}; \mathbf{h}, \mathbf{q}\right)\right]_{p_l}^{\mathcal{P}} \tag{10}$$

$$dh_l = -\frac{1}{2}a_l h_l dt + a_l^{\frac{1}{2}} dw_l + dv_l \tag{11}$$

$$dq_l = -\hat{\mu}_l(\mathbf{p}; \mathbf{h}, \mathbf{q})dt + dN_l, \quad \forall l = 1, \ldots, L. \tag{12}$$

In existing works, the convergence of the gradient algorithm in (9) and the throughput optimality of the MWQ in (4) are all based on an important assumption that the CSI and the QSI $(\mathbf{h}, \mathbf{q})$ remains constant during the algorithm iterations in (9). However, in practice, this may not be satisfied especially for fast fading channels and heavy traffic arrivals. In this paper, we are interested in studying the convergence behavior as well as the throughput and delay penalty of the iterative MWQ algorithm when the CSI and the QSI are changing at a similar timescale as that of the MWQ iterations.

C. Virtual Stochastic Dynamic Systems

In this subsection, we show that studying the convergence behavior of MWQ algorithm iterations in (9) and the queue stability can be transformed into an equivalent problem of *stochastic stability* in a
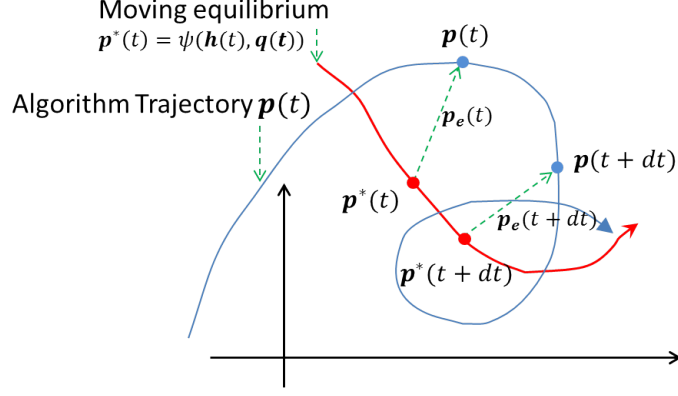
Figure 2. An illustration of the algorithm trajectory for solving an MWQ problem with time-varying CSI and QSI. The dynamics of the CSI and QSI excite the equilibrium $\mathbf{p}^*(t)$ to move around, and hence the convergence of $\mathbf{p}(t)$ is not guaranteed.

virtual stochastic dynamic system (VSDS). As a result of this association, we can focus on analyzing the behavior of the VSDS instead of the original complicated MWQ algorithm dynamics. We first have a few definitions.

Definition 2 (Equilibrium Point): Given the CSI and QSI parameter $(\mathbf{h}, \mathbf{q})$, $\mathbf{p}^*(\mathbf{h}, \mathbf{q})$ is called an equilibrium point of the MWQ algorithm dynamics in (9) if $\nabla \mathcal{L}(\mathbf{p}^*; \mathbf{h}, \mathbf{q}) = 0$. ∎

When the CSI and QSI $(\mathbf{h}, \mathbf{q})$ are quasi-static, the equilibrium point $\mathbf{p}^*(\mathbf{h}, \mathbf{q})$ is fixed and it has been shown [19], [20] that the MWQ algorithm iterations in (10) converges to $\mathbf{p}^*(\mathbf{h}, \mathbf{q})$ after sufficient iterations. However, when $(\mathbf{h}, \mathbf{q})$ are time-varying, the equilibrium point $\mathbf{p}^*(\mathbf{h}, \mathbf{q})$ is also time-varying as illustrated in Fig. 2 and it is not known if the MWQ iterations can track the *moving target*. To measure the tracking performance, we define the *tracking error vector* between the MWQ algorithm trajectory and the moving equilibrium point as below.

Definition 3 (Tracking Error Vector): The tracking error vector of the MWQ algorithm is a vector difference between the algorithm trajectory $\mathbf{p}(t)$ and the *target* equilibrium point $\mathbf{p}^*(\mathbf{h}(t), \mathbf{q}(t))$, i.e., $\mathbf{p}_e(t) = \mathbf{p}(t) - \mathbf{p}^*(t)$. ∎

For a notation convenience, let $\psi : (\mathbf{h}, \mathbf{q}) \mapsto \mathbf{p}^*(\mathbf{h}, \mathbf{q})$ be a mapping from the current CSI and QSI $(\mathbf{h}, \mathbf{q})$ to the equilibrium point $\mathbf{p}^*(\mathbf{h}, \mathbf{q})$. From Definition 3, the drift of the tracking error can be expressed as

$$
\begin{aligned}
d\mathbf{p}_e &= d\mathbf{p} - d\mathbf{p}^* \\
&= \kappa \left[\nabla \mathcal{L}(\mathbf{p}; \mathbf{h}, \mathbf{q}) \right]_{\mathbf{p}}^{\mathcal{P}} dt - \psi_q(\mathbf{h}, \mathbf{q}) d\mathbf{q} - \psi_h(\mathbf{h}, \mathbf{q}) d\mathbf{h}
\end{aligned}
\tag{13}
$$

where $\psi_q(\cdot) = \frac{\partial}{\partial \mathbf{q}} \psi(\mathbf{h}, \mathbf{q})$ and $\psi_h(\cdot) = \frac{\partial}{\partial \mathbf{h}} \psi(\mathbf{h}, \mathbf{q})$ are partial derivatives of the equilibrium point $\mathbf{p}^* = \psi(\mathbf{h}, \mathbf{q})$ over the current QSI $\mathbf{q}$ and CSI $\mathbf{h}$. They represent the sensitivity of $\mathbf{p}^*(\mathbf{h}, \mathbf{q})$ with

respect to the variations of the CSI and QSI $(\mathbf{h}, \mathbf{q})$. The terms $\psi_q(\mathbf{h}, \mathbf{q})d\mathbf{q}$ and $\psi_h(\mathbf{h}, \mathbf{q})d\mathbf{h}$ represent the change of the optimal power $d\mathbf{p}^*$ corresponding to the time-varying QSI $d\mathbf{q}(t)$ and CSI $d\mathbf{h}(t)$, respectively. Note that, as $\mathbf{h}$ is complex, $\psi_h(\mathbf{h}, \mathbf{q})d\mathbf{h}$ is defined as $\psi_{h_l} dh_l = \frac{\partial \psi}{\partial x_l} dx_l + \frac{\partial \psi}{\partial y_l} dy_l$, for each complex component[4] $h_l = x_l + iy_l$. Taking $\mathbf{p} = \mathbf{p}^* + \mathbf{p}_e$, we denote

$$f(\mathbf{p}_e; \mathbf{h}, \mathbf{q}) \triangleq \kappa \left[\nabla \mathcal{L} \left(\mathbf{p}_e + \mathbf{p}^*; \mathbf{h}, \mathbf{q} \right) \right]_{\mathbf{p}_e + \mathbf{p}^*}^{\mathcal{P}}$$

as a mapping of the gradient iterations. Using the system dynamics of $\mathbf{h}(t)$ and $\mathbf{q}(t)$ in (11)-(12), we construct a *stochastic error dynamic system* to describe the tracking error process $\mathbf{p}_e(t)$ as follows.

Definition 4 (Stochastic Error Dynamic System (SEDS)): The stochastic error dynamic system is characterized by the following SDE

$$d\mathbf{p}_e = f_e(\mathbf{p}_e; \mathbf{h}, \mathbf{q})dt + b_e(\mathbf{p}_e; \mathbf{h}, \mathbf{q})d\mathbf{N}(t) + c_e(\mathbf{p}_e; d\mathbf{W}(t), d\mathbf{V}(t)) \tag{14}$$

where $f_e(\mathbf{p}_e; \mathbf{h}, \mathbf{q}) = f(\mathbf{p}_e; \mathbf{h}, \mathbf{q}) - \psi_q(\textbf{.})\hat{\boldsymbol{\mu}}(\textbf{.}) + \frac{1}{2}\psi_h(\textbf{.})A\mathbf{h}$, $b_e(\textbf{.}) = -\psi_q(\textbf{.})$, and $c_e(\textbf{.}) = -\psi_h(\textbf{.})(A^{\frac{1}{2}}d\mathbf{W}(t) + d\mathbf{V}(t))$. $A = \text{diag}\{a_1, \ldots, a_L\}$ is a matrix of CSI correlation coefficient in (2). ∎

It is known that when the CSI and QSI $(\mathbf{h}, \mathbf{q})$ are static, the MWQ algorithm trajectory always converges to the static equilibrium point $\mathbf{p}^*(\mathbf{h}, \mathbf{q})$. However, when the CSI and QSI are time-varying in a similar timescale as the MWQ algorithm iterations, the algorithm convergence is not obvious. To study the behavior of the algorithm dynamics induced by the time-varying CSI and QSI, we construct a Virtual Stochastic Dynamic System (VSDS), which combines the overall dynamics of the CSI and QSI in (11) and (12) with the Stochastic Error Dynamic System (SEDS) in (14) as follows.

Definition 5 (Virtual Stochastic Dynamic System (VSDS)): Let $\mathbf{z} = (\mathbf{p}_e, \mathbf{h}, \mathbf{q})$ be a joint system state. The virtual stochastic dynamic system is characterized by the following coupled SDE,

$$\mathcal{Z}: \qquad d\mathbf{z} = F(\mathbf{z})dt + B(\mathbf{z})d\mathbf{N} + C(\mathbf{z}, d\mathbf{W}, d\mathbf{V}) \tag{15}$$

where

$$F(\mathbf{z}) = \begin{bmatrix} f(\mathbf{p}_e; \mathbf{h}, \mathbf{q}) - \psi_q \hat{\boldsymbol{\mu}}(\mathbf{p}_e + \mathbf{p}^*) + \frac{1}{2}\psi_h A\mathbf{h} \\ -\frac{1}{2}A\mathbf{h} \\ -\hat{\boldsymbol{\mu}}(\mathbf{p}_e + \mathbf{p}^*) \end{bmatrix}$$

$$B(\mathbf{z}) = \begin{bmatrix} -\psi_q(\mathbf{h}, \mathbf{q}) \\ \mathbf{0}_{2L \times L} \\ \mathbf{I}_L \end{bmatrix} \quad \text{and} \quad C(\mathbf{z}, d\mathbf{W}(t)) = \begin{bmatrix} -\psi_h(\mathbf{h}, \mathbf{q})(A^{\frac{1}{2}}d\mathbf{W} + d\mathbf{V}) \\ A^{\frac{1}{2}}d\mathbf{W} + d\mathbf{V} \\ \mathbf{0}_L \end{bmatrix}.$$

∎

---

[4]The complex derivative for a real value function $\psi(h)$ is defined as $\frac{\partial \psi}{\partial h} = \frac{1}{2} \left(\frac{\partial \psi}{\partial x} - i\frac{\partial \psi}{\partial y} \right)$ and $\frac{\partial \psi}{\partial \bar{h}} = \frac{1}{2} \left(\frac{\partial \psi}{\partial x} + i\frac{\partial \psi}{\partial y} \right)$, for $h = x + iy$. The Taylor expansion of $\psi(h)$ is thus given by $d\psi = \frac{\partial \psi}{\partial h} dh + \frac{\partial \psi}{\partial \bar{h}} d\bar{h} = \frac{\partial \psi}{\partial x} dx + \frac{\partial \psi}{\partial y} dy$ [21].
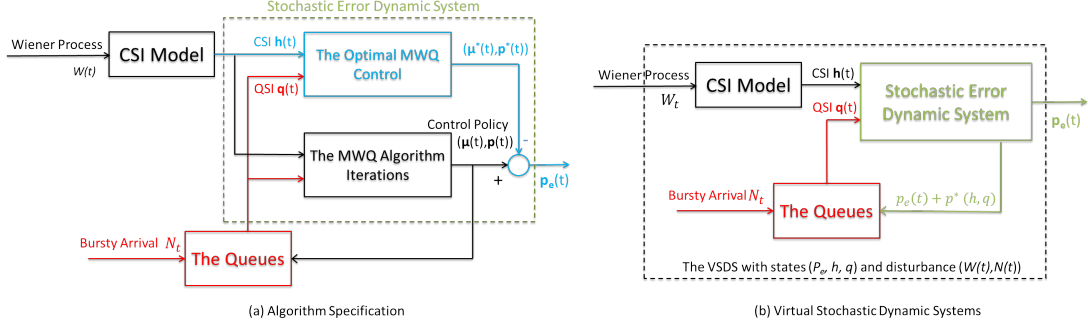
Figure 3. An illustration of the connection between the MWQ algorithm dynamics and Virtual Stochastic Dynamic System (VSDS). Fig. (a) illustrates the dynamics in the MWQ algorithm domain. The control policies $(\boldsymbol{\mu}(t), \mathbf{p}(t))$ from the MWQ algorithm iterations are driven by the CSI dynamics $\mathbf{h}(t)$ and the QSI dynamics $\mathbf{q}(t)$. Fig. (b) illustrates the coupled MWQ iterations, CSI and QSI from the VSDS perspective, where the power tracking error $\mathbf{p}_e(t)$, the CSI and QSI $(\mathbf{h}(t), \mathbf{q}(t))$ are modeled as a joint state of the SDE, which is driven by external stochastic processes W_t and N_t.

Fig. 3 illustrates the inter-connection between the key components in the VSDS. Fig. 3(a) illustrates the dynamics in the MWQ algorithm domain. Specifically the queueing dynamics $\mathbf{q}(t)$ is driven by the bursty arrival process $\mathbf{N}(t)$ as well as the control policy $(\boldsymbol{\mu}(t), \mathbf{p}(t))$. At the same time, the control actions $(\boldsymbol{\mu}(t), \mathbf{p}(t))$ are driven by the MWQ algorithm iterations, which depend on the CSI $\mathbf{h}(t)$ and the QSI $\mathbf{q}(t)$. Fig. 3(b) illustrates the dynamics in the VSDS domain. The system consists of the SEDS (driving the tracking error process $\mathbf{p}_e(t) = \mathbf{p}(t) - \mathbf{p}^*(t)$) as well as the CSI $\mathbf{h}(t)$ and QSI $\mathbf{q}(t)$ driven by external processes $\mathbf{W}(t)$ and $\mathbf{N}(t)$.

We show in the following theorem that, studying the convergence behavior of the MWQ algorithm (9) is the same as studying the stability property of the VSDS in (15). Also, evaluating the stability of queue backlogs driven by the MWQ algorithm dynamics is equivalent to investigating the stability property of the system state $\mathbf{z}(t)$ in the VSDS.

Theorem 1 (Connections between the MWQ Algorithm Dynamics and the VSDS): The actual queue trajectory of the MWQ algorithm in (12) is the same as the solution process $\mathbf{q}(t)$ in the VSDS in (15). Furthermore, the power control trajectory of the MWQ algorithm in (10) converges to the equilibrium $\mathbf{p}^*(\mathbf{h}, \mathbf{q})$ if and only if the SDE in (14) is globally asymptotically stable at $\mathbf{p}_e = \mathbf{0}$, i.e., given any initial state $\mathbf{p}_e(0) \in \mathbb{R}_+^L$, $\lim_{t \to \infty} \Pr(\mathbf{p}_e(t) = 0) = 1$. ∎

Proof: Please refer to Appendix A for the proof. ∎

As a result of Theorem 1, we can focus on the VSDS dynamics in order to study the delay performance penalty of MWQ due to time varying CSI and QSI. Nevertheless, due to the mutual coupling of the SDEs in the VSDS, it is still difficult to study its stability behavior. In the rest of the paper, we will focus on extending the stochastic Foster-Lyapunov method [22] to derive the stochastic stability results of the VSDS.

III. Performance Analysis of MWQ Algorithm under Time-Varying Arrivals and Channels

In this section, we shall analyze the tracking performance of the MWQ algorithm under time-varying channels. We bridge the connection between the property of the Lyapunov stochastic drift and the stochastic stability of the corresponding VSDS. Following this result, we then derive an expected queue bound under the MWQ algorithm in time-varying channels.

A. Stochastic Stability of Random Process

Let $\mathbf{z} = (\mathbf{p}_e, \mathbf{h}, \mathbf{q})$ be a joint state of the VSDS in (15), where $\mathbf{p}_e$ is the tracking error, $\mathbf{h}$ is the channel coefficient and $\mathbf{q}$ is the queue backlog. Denote $\mathbf{z}(t)$ as the stochastic process starting from $t = 0$ with initial state $\mathbf{z}(0)$. We have the following definition of stochastic stability to characterize the behavior of $\mathbf{z}(t)$.

Definition 6 (Stochastic Stability): Given any initial state $\mathbf{z}(0) \in \mathcal{Z}$, the stochastic process $\mathbf{z}(t)$ is globally stochastically stable, if there exists $0 \leq D < \infty$, such that

$$\limsup_{t \to \infty} \frac{1}{t} \int_0^t \mathbb{E} \|\mathbf{z}(t)\| \leq D.$$

■

Notice that this definition is analogue to the usual concept of *stability* in *deterministic* system [23], whereas, the condition here is taken over a time averaged expectation. This general criteria can be applied to a non-stationary process, such as a queueing system with different classes of services. In fact, in this work, we do not require the queue dynamics and the MWQ algorithm trajectory to be stationary.

Define a Lyapunov function of the state $\mathbf{z}(t)$ as $V(\mathbf{z}) = \mathbf{z}^H \mathbf{z}$. We can investigate the evolution of the Lyapunov function by studying its drift along the state trajectory. Analogue to the discrete-time one-step *conditional Lyapunov drift* in [5], we define the continuous time Lyapunov drift generator as

$$LV(\mathbf{z}(t)) = \lim_{\delta \downarrow 0} \frac{\mathbb{E}\left[V(\mathbf{z}(t+\delta)) - V(\mathbf{z}(t))|\mathbf{z}(t)\right]}{\delta} \tag{16}$$

where the expectation (conditioned on the current state $\mathbf{z}(t)$) is taken over the randomness of the CSI and the arrival to the QSI. The Lyapunov drift represents the expected evolving direction of the Lyapunov function $V(\mathbf{z})$ from the current state $\mathbf{z}(t)$, and $LV(\mathbf{z})$ is called an *infinitesimal estimator* of $V(\mathbf{z})$. As $V(\mathbf{z})$ is a norm-like function [23], the boundedness of the Lyapunov function implies the boundedness of state $\mathbf{z}(t)$ and the dynamics of the Lyapunov function reveals the evolution of state $\mathbf{z}(t)$. For example, when the drift is negative, $\|\mathbf{z}(t)\|$ is most likely decreasing. The Lyapunov drift $LV(\mathbf{z})$ can also be derived from the SDE of $\mathbf{z}(t)$ as stated in the following lemma.

Lemma 2 (Continuous-Time Lyapunov Drift [24]): Suppose that there is a d-dimensional stochastic process $\mathbf{z}(t)$ described by a SDE

$$d\mathbf{z} = f(\mathbf{z})dt + g(\mathbf{z})d\mathbf{W} + h(\mathbf{z})d\mathbf{N}$$

where $\mathbf{W}(t) \in \mathbb{C}^L$ is a standard complex Wiener process and $\mathbf{N}(t) = (N_1(t), \ldots, N_L(t)) \in \mathbb{Z}_+^L$ is a Poisson process with intensities λ_l, $l = 1, \ldots, L$. For any given Lyapunov function $V(\mathbf{z}) \in \mathcal{C}^2 :$ $\mathcal{Z} \to \mathbb{R}_+$ that has compact support [24], the stochastic Lyapunov drift can be written as

$$
\begin{aligned}
LV(\mathbf{z}) &= 2\frac{\partial V(\mathbf{z})}{\partial \mathbf{z}}f(\mathbf{z}) + \frac{1}{2}\mathrm{tr}\left[g(\mathbf{z})^H\frac{\partial^2 V(\mathbf{z})}{\partial \overline{\mathbf{z}}\partial \mathbf{z}}g(\mathbf{z}) + g(\mathbf{z})\frac{\partial^2 V(\mathbf{z})}{\partial \mathbf{z}\partial \overline{\mathbf{z}}}g(\mathbf{z})^H\right] \\
&\quad + \sum_{l=1}^{L_2}\lambda_l\left(V(\mathbf{z} + h^{(l)}(\mathbf{z})) - V(\mathbf{z})\right)
\end{aligned}
$$

where $h^{(l)}(\mathbf{z})$ is the l-th column of $h(\mathbf{z})$. ∎

The above lemma establishes a connection between the infinitesimal estimator $LV(\mathbf{z})$ and the specific SDE. The proof is similar to that in [24] with a notation extension to complex variables [21]. By exploiting the property of the Lyapunov drift, we can characterize the stochastic stability of random process $\mathbf{z}(t)$ described by the SDE in (15). We summarize the result in the following theorem.

Theorem 2 (Stochastic Stability from Lyapunov Drift): Suppose the stochastic Lyapunov drift of the process $\mathbf{z}(t)$ satisfies

$$LV(\mathbf{z}) \leq -a\|\mathbf{z}\| + g(\mathbf{s}) \tag{17}$$

for all $\mathbf{z} \in \mathcal{Z}$, where a is some positive constant and $\mathbf{s}(t)$ is a stochastic process that satisfies

$$\limsup_{t\to\infty}\frac{1}{t}\int_0^t \mathbb{E}\left[g(\mathbf{s}(\tau))\right]d\tau \leq d$$

for some function $g : \mathbf{s} \mapsto \mathbb{R}$ and $d < \infty$. Then the process $\mathbf{z}(t)$ is stochastically stable, and

$$\limsup_{t\to\infty}\frac{1}{t}\int_0^t \mathbb{E}\|\mathbf{z}(\tau)\|d\tau \leq \frac{d}{a}.$$

∎

Proof: Please refer to Appendix B for the proof. ∎

The above result is an extension of the Foster-Lyapunov criteria for continuous time processes in [22]. If $\mathbf{z}(t)$ is a system state that relates to the queue length and the tracking error of the power variable, the stochastic stability forms an estimation on the queue bound as well as the power penalty due to the time-varying parameters. The advantage of the Foster-Lyapunov method enables a qualitative analysis of the VSDS without explicitly solving the SDE. In the following, we shall illustrate how to construct a Lyapunov drift for the VSDS.

B. Stability Analysis of the MWQ Algorithm

In this section, we shall apply the stochastic stability analysis method to study the stability of the VSDS (15). Specifically, according to Lemma 2, the Lyapunov drift for the VSDS (15) is given by[5]

$$
\begin{aligned}
LV(\mathbf{z}) &= 2\mathbf{z}^H F(\mathbf{z}) + \frac{1}{2}\text{tr}\left[2C(\mathbf{z},\text{.})^H C(\mathbf{z},\text{.})\right] + \sum_{l=1}^{L}\lambda_l\left[V(\mathbf{z}+B^{(l)}) - V(\mathbf{z})\right] \\
&\leq 2\mathbf{p}_e^T f(\mathbf{p}_e;\mathbf{h},\mathbf{q}) - 2\mathbf{p}_e^T \psi_q(\mathbf{h},\mathbf{q})\hat{\boldsymbol{\mu}}(\mathbf{p}_e+\mathbf{p}^*) + \mathbf{p}_e^T \psi_h(\mathbf{h},\mathbf{q})A\mathbf{h} \\
&\quad -\mathbf{h}^H A\mathbf{h} - 2\mathbf{p}_e^T \psi_q(\mathbf{h},\mathbf{q})\boldsymbol{\lambda} - 2\sum_{l=1}^{L} q_l\left[\hat{\mu}_l(\mathbf{p}_e+\mathbf{p}^*) - \lambda_l\right] \\
&\quad +\text{tr}\left(2\left(A^{\frac{1}{2}}\right)^T \psi_h^H \psi_h A^{\frac{1}{2}} + \psi_q^T \psi_q\right) + \sum_{l=1}^{L}(2a_l+\lambda_l)
\end{aligned}
\tag{18}
$$

where $B^{(l)}$ stands for the l-th column of $B(\mathbf{z})$ and $\Lambda = \text{diag}\{\lambda_1,\ldots,\lambda_L\}$ is the arrival matrix.

As illustrated in Theorem 2, negative drift terms in $LV(\mathbf{z})$ are desirable because they can drive the stochastic state process towards the origin and contribute to stabilization of the VSDS. In the following, we shall analyze the key terms on the R.H.S. of (18) and discuss their contributions. Intuitively, a fast MWQ algorithm and a high transmission rate can contribute to driving the $LV(\mathbf{z})$ negative and we shall elaborate on such properties in the following.

We first define the following, which will be used throughout the analysis. Let $S_{\min}(t) = \min_l\left\{|h_l(t)|^2\right\}$ and $S_{\max}(t) = \max_l\left\{|h_l(t)|^2\right\}$ be the minimum and maximum channel gains among L transmission links at time t, respectively. Notice that $|h_l|^2$ has stationary distributions and we denote its cumulative distribution function as $F_h(x)$. Thus $S_{\min}$ and $S_{\max}$ are also ergodic processes with stationary distributions given by the L-th *order statistics* as $F_S^{\min}(s) = \text{P}(S_{\min} \leq s) = 1 - \left[1 - \text{P}\left(|h|^2 \leq s\right)\right]^L = 1 - [1 - F_h(s)]^L$ and $F_S^{\max}(s) = \text{P}\left(S_{\max} \leq s\right) = \text{P}\left(|h|^2 \leq s\right)^L = F_h(s)^L$.

The following lemma summarizes the contribution of the convergence speed of the MWQ iterations in (9) to the drift $LV(\mathbf{z})$ in (18).

Lemma 3 (Negative Drift Contribution of Convergence Speed in MWQ Gradient Iteration): Given any CSI and QSI realizations $\mathbf{h}(t) = \mathbf{h}$ and $\mathbf{q}(t) = \mathbf{q} \succ \mathbf{1}$, there exists $\alpha(S_{\min}, S_{\max}) > 0$ that satisfies[6]

$$
\mathbf{p}_e^T f(\mathbf{p}_e;\mathbf{h},\mathbf{q}) \leq -\kappa\alpha\|\mathbf{p}_e\|^2
\tag{19}
$$

for all $t \geq 0$, where κ is the step size parameter of the MWQ iterations in (9). ∎

Proof: Please refer to Appendix C for the proof. ∎

---

[5]Note that Lemma 2 does not specify the drift for the term $d\mathbf{V}$. However, as the reflection $|d\mathbf{V}| \leq |A^{\frac{1}{2}}d\mathbf{W}|$, we can treat $\mathbf{V}(t)$ as $A^{\frac{1}{2}}\mathbf{W}(t)$ and yield an upper bound for $LV(\mathbf{z})$.

[6]For vectors $\mathbf{a} = (a_1, a_2, \ldots, a_L)$ and $\mathbf{b} = (b_1, b_2, \ldots, b_L)$, $\mathbf{a} \succ \mathbf{b}$ is defined as $a_i > b_i, \forall i = 1, \ldots, L$.

This lemma illustrates that the tracking error term $\mathbf{p}_e$ contributes to the negative drift (proportional to $\kappa\alpha$) in $LV(\mathbf{z})$ in (18). The larger the tracking error $\|\mathbf{p}_e\|$ is, the stronger force the MWQ iterations will drag the system state $\mathbf{p}$ to the optimal $\mathbf{p}^*$, which in turn helps the stabilization of the system. In fact, the negative drift depends on the MWQ iteration step size κ, which controls the *convergence rate*[7] of the MWQ iterations under static $\mathbf{h}$ and $\mathbf{q}$.

From the Lyapunov drift for VSDS in (18), the transmission rate $\hat{\boldsymbol{\mu}}(t)$ also contributes to negative drift in (18), which in turns help to stabilize the VSDS. Before we quantify the negative drift contribution, we first discuss several structural properties of the transmission rate at the equilibrium. Let $\boldsymbol{\mu}^*(\mathbf{h},\mathbf{q}) = \hat{\boldsymbol{\mu}}(\mathbf{p}^*(\mathbf{h},\mathbf{q});\mathbf{h},\mathbf{q})$ be the transmission rate at the equilibrium point $\mathbf{p}^*(\mathbf{h},\mathbf{q})$ (optimal transmission rate under the MWQ policy). We have the following lemmas about the structural property of $\boldsymbol{\mu}^*(\mathbf{h},\mathbf{q})$ and the actual transmission rate $\hat{\boldsymbol{\mu}}(t)$.

Lemma 4 (Structural Properties of the Transmission Rate at Equilibrium): The transmission rate $\boldsymbol{\mu}^*(\mathbf{h},\mathbf{q})$ at the equilibrium $\mathbf{p}^*(\mathbf{h},\mathbf{q})$ of the VSDS has the following properties,

$$\sum_{l=1}^{L} q_l \mu_l^*(\mathbf{h},\mathbf{q}) \geq \|\mathbf{q}\| \min\left\{ \log\left(\frac{S_{\min}}{V}\|\mathbf{q}\|\right), L\lambda_{\max} + \log\frac{S_{\min}}{|h_0|^2} \right\} \tag{20}$$

and

$$\frac{1}{L} \min\left\{ \log\left(\frac{S_{\min}}{V}\|\mathbf{q}\|\right), L\lambda_{\max} + \log\frac{S_{\min}}{|h_0|^2} \right\} \leq \|\boldsymbol{\mu}^*(\mathbf{h},\mathbf{q})\| \leq \log\left(\frac{S_{\max}}{V}\|\mathbf{q}\|\right) \tag{21}$$

for $\|\mathbf{q}\|S_{\min} > V$. ∎

Proof: Please refer to Appendix D for the proof. ∎

Lemma 5 (Structural Properties of the Actual Rate $\hat{\boldsymbol{\mu}}(t)$): There exists a $\beta > 0$ depending on $S_{\min}$ and $S_{\max}$, such that, for all $t \geq 0$, the actual transmission rate at time t, $\hat{\boldsymbol{\mu}}(t) = \hat{\boldsymbol{\mu}}(\mathbf{p}(t);\mathbf{h}(t),\mathbf{q}(t))$ satisfies

$$\|\boldsymbol{\mu}^*(\mathbf{h}(t),\mathbf{q}(t))\| - \log\left(1+\beta\|\mathbf{p}_e(t)\|\right) \leq \|\hat{\boldsymbol{\mu}}(t)\| \leq \|\boldsymbol{\mu}^*(\mathbf{h}(t),\mathbf{q}(t))\| + \log\left(1+\beta\|\mathbf{p}_e(t)\|\right). \tag{22}$$

∎

Proof: Please refer to Appendix E for the proof. ∎

Lemma 4 shows that the term $\sum q_l \mu_l^*$ grows faster than $\|\mathbf{q}\|$ and $\|\boldsymbol{\mu}^*(\mathbf{h},\mathbf{q})\|$ is lower bounded with the order $\log(\|\mathbf{q}\|)$. On the other hand, Lemma 5 illustrates that, although there is a tracking error $\mathbf{p}_e$ in the power allocation, a minimum transmission rate is still guaranteed and the rate penalty due to the tracking error $\mathbf{p}_e$ is no larger than $\log(1+\beta\|\mathbf{p}_e\|)$.

---

[7]Note that the MWQ iteration in (9) is expressed in continuous time and a larger κ is always desirable from the perspective of convergence speed. However, in practice, the MWQ iterations are implemented in discrete time and the corresponding discrete time step size is given by $\kappa\tau$ where τ is the slot duration of iterations. For a given τ, a large κ will speed up the iteration but also contributes to a larger *steady state errors* of $\mathcal{O}(\kappa\tau)$ in the discrete time iterations.

Based on the properties in Lemma 4-5, we can derive an upper bound of the Lyapunov drift in (18). Let $a_A = \|A\| = \max\{a_l\}$ be the CSI fading rate parameter, where A is the coefficient matrix of the CSI dynamics defined in (2). Let $\lambda_{\max} = \|\Lambda\| = \max_l\{\lambda_l\}$ be the maximum arrival rate among all the transmission links.

Lemma 6 (Lyapunov Drift Property for VSDS): Suppose there exists constants $\gamma_q < \infty$ and $\gamma_h < \infty$, such that $\|\psi_q(\mathbf{h}(t), \mathbf{q}(t))\| \leq \gamma_q$, $\|\psi_h(\mathbf{h}(t), \mathbf{q}(t))\| \leq \gamma_h$, for all $t \geq 0$. In addition, the step size κ satisfies $\kappa > \frac{2}{\alpha}\max\{\gamma_q^2, \beta\gamma_q\}$ under all $\mathbf{h}(t)$. Then the stochastic Lyapunov drift in (18) is bounded by

$$LV \quad \leq \quad -(\|\mathbf{p}_e\| + \|\mathbf{q}\| + \|\mathbf{h}\|) + D(S_{\min}, S_{\max}) \tag{23}$$

where

$$D(S_{\min}, S_{\max}) \quad = \quad L(2a_A(1 + \gamma_h^2) + \gamma_q^2 + \lambda_{\max}) + \frac{1}{8a_A[1 - \gamma_h^2 a_A/(\kappa\alpha)]}$$
$$+ \frac{2\gamma_q^2\lambda_{\max}^2}{\kappa\alpha} + \frac{V}{S_{\min}}2^{L\lambda_{\max}-1} + g(S_{\min}, S_{\max}) + C$$

and $g(S_{\min}, S_{\max})$ is a function bounded for all $S_{\min}$ and $S_{\max}$. ∎

Proof: Please refer to Appendix F for the proof. ∎

From the above lemma, the Lyapunov drift (18) is increasingly negative for sufficiently large $\|\mathbf{q}\|$ and $\|\mathbf{h}\|$ and this *negative drift* drives the system state back to a trajectory with bounded norm. This property stabilizes the VSDS. Denote $\overline{\alpha}_0 = \mathbb{E}\left[\frac{1}{\alpha}\right]$, $\overline{\gamma}_0 = \mathbb{E}\left[\frac{1}{8[1 - \gamma_h^2 a_A/(\kappa\alpha)]}\right]$, $\overline{\sigma} = \mathbb{E}[\frac{1}{S_{\min}}]$ and $\overline{g} = \mathbb{E}[g(S_{\min}, S_{\max})]$. Note that as $S_{\min}$ and $S_{\max}$ are the L-th order statistics of stationary processes $|h_l|^2$, $\overline{\sigma}$ and $\overline{g}$ are bounded above. The stability results of the VSDS can be summarized as follows.

Theorem 3 (Stability of the VSDS): The system state $\mathbf{z}(t)$ of VSDS in (15) is stochastically stable and satisfies

$$\limsup_{t\to\infty} \frac{1}{t}\int_0^t \mathbb{E}\left[\|\mathbf{z}(\tau)\|\right] d\tau \leq L(2a_A(1+\gamma_h^2)+\gamma_q^2+\lambda_{\max}) + \frac{\overline{\gamma}_0}{a_A} + \frac{\overline{\alpha}_0\gamma_q^2\lambda_{\max}^2}{\kappa} + V2^{L\lambda_{\max}-1}\overline{\sigma}+\overline{g}. \tag{24}$$

∎

The above theorem is a direct result of Lemma 6 and Theorem 2. As $\|\mathbf{q}\| \leq \|\mathbf{z}\|$, we can obtain the average queue bound from the following corollary.

Corollary 1 (Expected Average Queue Bound under Time-varying CSI and QSI): The expected average queue bound under MWQ algorithm in time-varying CSI and QSI is given by

$$\limsup_{t\to\infty} \frac{1}{t}\int_0^t \mathbb{E}\left[\|\mathbf{q}(\tau)\|\right] d\tau \leq L(2a_A(1+\gamma_h^2)+\gamma_q^2+\lambda_{\max}) + \frac{\overline{\gamma}_0}{a_A} + \frac{\overline{\alpha}_0\gamma_q^2\lambda_{\max}^2}{\kappa} + V2^{L\lambda_{\max}-1}\overline{\sigma}+\overline{g}. \tag{25}$$

∎

The result shows the upper bound of the average worst case queue (corresponding to the worst case delay) of the network. The bound depends on several important parameters, namely the CSI fading rate a_A, and the sensitivities of the equilibrium $\mathbf{p}^*(\mathbf{h}, \mathbf{q})$ w.r.t. $\mathbf{h}$ and $\mathbf{q}$, (γ_h, γ_q).
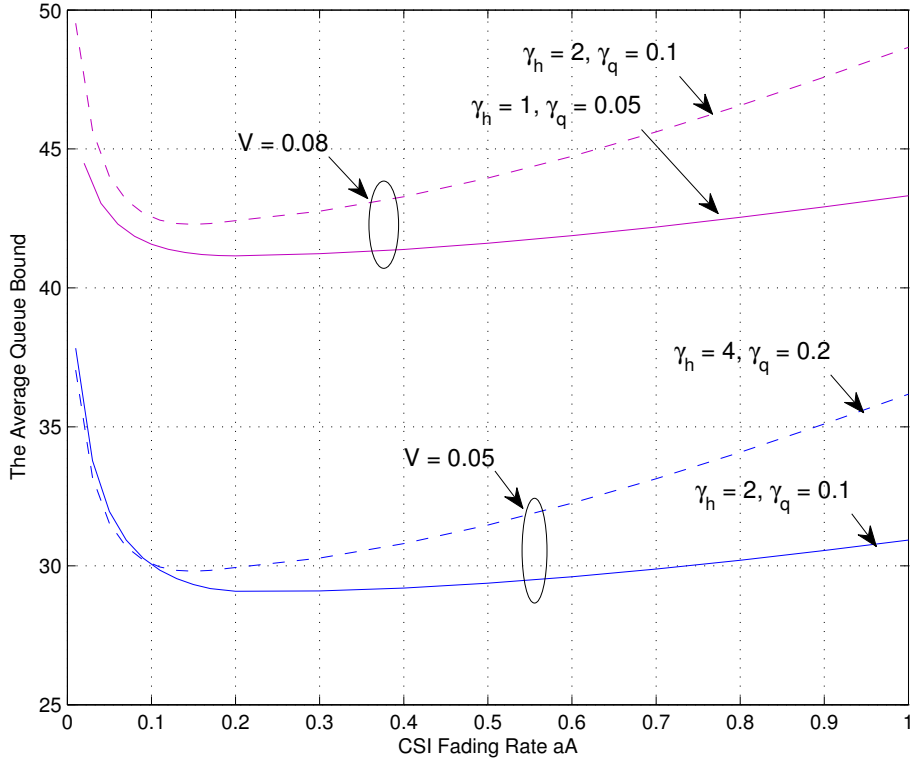
Figure 4. A numerical illustration of the average queue bound (for the worst queue) in (25) versus the CSI fading rate a_A. The numerical result is under $L = 4$ links and maximum arrival rate $\lambda_{\max} = 1$, and different assumptions of sensitivity parameters γ_h and γ_q. The numerical queue bound is increasing with the CSI fading rate a_A, the parameters γ_h and γ_q.

Fig. 4 gives a numerical illustration of the theoretical queue bound in (25) under $L = 4$ links, maximum arrival rate $\lambda_{\max} = 1$, various CSI fading rates a_A, and sensitivity parameters γ_h and γ_q. Note that the delay bound increases w.r.t. γ_h and γ_q. Note that the delay bound increases w.r.t. γ_h, γ_q and at both large and small fading speed (a_A). For large a_A, there is the penalty of the increased tracking error due to time varying CSI. For small a_l, the delay increases because the CSI may be stuck at a poor state for quite a long time.

IV. ADAPTIVE COMPENSATION FOR THE MWQ ALGORITHM IN TIME-VARYING ARRIVALS AND CHANNELS

Based on the stochastic dynamics modeled by the VSDS, we consider modifying the gradient MWQ iterations in (9) to reduce the penalty induced by time varying CSI and QSI. Specifically, we introduce a *compensation term* to improve the stochastic dynamics of the VSDS in (15). This corresponds to a *compensation* term in the MWQ algorithm to offset the effect from the time-varying CSI and QSI. The overall compensated MWQ algorithm is shown to have a better convergence robustness w.r.t.

time varying CSI and QSI both analytically and numerically.

A. A Proposed Algorithm with Compensation Term

We have shown in Section II-C that the dynamics of tracking error $\mathbf{p}_e(t)$ can be modeled by a stochastic error dynamic system in (14), which consists of a drift term $f_e(\textbf{.})$ and diffusion terms $b_e(\textbf{.})$ and $c_e(\textbf{.}; d\mathbf{W})$. Without the diffusion terms, the SEDS eventually converges to the origin, as $f_e(\textbf{.})$ contributes a negative drift to the infinitesimal estimator $LV(\mathbf{p}_e)$, where we define the Lyapunov function as $V(\mathbf{p}_e) = \mathbf{p}_e^T \mathbf{p}_e$. However, with the presence of the diffusion terms, the system $d\mathbf{p}_e = f_e(\mathbf{p}_e; \mathbf{h}, \mathbf{q})dt$ is disturbed from the equilibrium at $\mathbf{p}_e = \mathbf{0}$ and the state $\mathbf{p}_e$ is driven away from the origin. The magnitude of $b_e(\textbf{.})$ and $c_e(\textbf{.})$ reflect the chance and intensity that the state $\mathbf{p}_e(t)$ is being disturbed. Based on this observation, one way to stabilize $\mathbf{p}_e(t)$ is to offset the diffusion terms $b_e(\textbf{.})$ and $c_e(\textbf{.})$ in the SEDS dynamics in (14). Equivalently, this corresponds to modifying the MWQ algorithm iterations in (9) to compensate for the effects of time varying CSI and QSI. From the error tracking vector $d\mathbf{p}_e$ in (13), we would like to compensate the movement of the optimal target $d\mathbf{p}^*(t)$ so that the resulting SEDS becomes $d\mathbf{p}_e = \kappa \left[\nabla\mathcal{L} \left(\mathbf{p}_e + \mathbf{p}^*; \mathbf{h}, \mathbf{q} \right) \right]_{\mathbf{p}_e}^{\mathcal{P}} dt$. In this ideal case, the $\mathbf{p}_e$ will converge to $\mathbf{0}$. However, the challenge is that we do not have an exact expression for $d\mathbf{p}^*(t)$ during the iteration because we do not have closed form expression of the equilibrium $\mathbf{p}^*(t)$. We shall propose an indirect method of estimating the compensation term.

Since the MWQ problem in (8) is convex, $\mathbf{p}^*$ is the optimum if and only if there exists $\boldsymbol{\lambda}^* \succeq \mathbf{0}$, such that

$$\nabla\mathcal{L}(\mathbf{p}^*; \mathbf{h}, \mathbf{q}) + \boldsymbol{\lambda}^* = \mathbf{0} \tag{26}$$

$$\lambda_l^* p_l^* = 0 \quad \forall l = 1, \ldots, L. \tag{27}$$

We denote the above system of equations (KKT conditions) as $\Phi(\mathbf{x}^*; \mathbf{h}, \mathbf{q}) = \mathbf{0}$, where $\mathbf{x}^* = (\mathbf{p}^*, \boldsymbol{\lambda}^*)$. Note that $\mathbf{x}^*$ is unique for a convex problem. Using implicit function theorem and assuming $\frac{\partial\Phi}{\partial\mathbf{x}^*}$ is non-singular, we have

$$d\mathbf{x}^* = \begin{bmatrix} d\mathbf{p}^* \\ d\boldsymbol{\lambda}^* \end{bmatrix} = -\left(\frac{\partial\Phi}{\partial\mathbf{x}^*}\right)^{-1} \frac{\partial\Phi}{\partial\mathbf{q}} d\mathbf{q} - 2\mathrm{Re}\left[\left(\frac{\partial\Phi}{\partial\mathbf{x}^*}\right)^{-1} \frac{\partial\Phi}{\partial\mathbf{h}} d\mathbf{h}\right]. \tag{28}$$

As a result, we obtain $d\mathbf{p}^* = \hat{\varphi}_q(\mathbf{p}^*, \boldsymbol{\lambda}(\mathbf{p}); \mathbf{h}, \mathbf{q})d\mathbf{q} + \mathrm{Re}\left[\hat{\varphi}_h(\mathbf{p}^*, \boldsymbol{\lambda}(\mathbf{p}); \mathbf{h}, \mathbf{q})d\mathbf{h}\right]$, where the vector-valued functions $\hat{\varphi}_q(\mathbf{p}^*; \textbf{.})$ and $\hat{\varphi}_h(\mathbf{p}^*; \textbf{.})$ are the rows for primal variable $d\mathbf{p}^*$ from $-\left(\frac{\partial\Phi}{\partial\mathbf{x}^*}\right)^{-1} \frac{\partial\Phi}{\partial\mathbf{q}}$ and $-2\left(\frac{\partial\Phi}{\partial\mathbf{x}^*}\right)^{-1} \frac{\partial\Phi}{\partial\mathbf{h}}$ in (28), respectively. Thus the MWQ iterations with compensation is given by

$$\dot{\mathbf{p}} = \left[\kappa\nabla\mathcal{L}(\mathbf{p}; \mathbf{h}(t), \mathbf{q}(t)) - \hat{\varphi}_q(\mathbf{p}, \boldsymbol{\lambda}(\mathbf{p}); \mathbf{h}(t), \mathbf{q}(t))d\mathbf{q} - \mathrm{Re}\left[\hat{\varphi}_h(\mathbf{p}, \boldsymbol{\lambda}(\mathbf{p}); \mathbf{h}(t), \mathbf{q}(t))d\mathbf{h}\right] \right]_{\mathbf{p}}^{\mathcal{P}} \tag{29}$$

where $\hat{\varphi}_q(\textbf{.})d\mathbf{q}$ and $\mathrm{Re}\left[\hat{\varphi}_h(\textbf{.})d\mathbf{h}\right]$ are compensation terms. Here, we use the current algorithm state $\mathbf{p}(t)$ as an approximation of the target equilibrium $\mathbf{p}^*(t)$ and $\boldsymbol{\lambda}$ is computed via the KKT conditions

in (26)-(27). The compensation term can be interpreted as an estimation on how the target equilibrium $\mathbf{p}^*$ is moving according to the time-varying CSI and QSI $(d\mathbf{h}, d\mathbf{q})$. When $\mathbf{p}$ is close to $\mathbf{p}^*$ (i.e., $\mathbf{p}_e$ is small), the estimation $\hat{\varphi}(\mathbf{p}, \boldsymbol{\lambda}(\mathbf{p}); d\mathbf{h}, d\mathbf{q})$ on $d\mathbf{p}^*$ is accurate. Thus the compensation term helps further reduce the tracking error and the algorithm would eventually converge to the equilibrium $\mathbf{p}^*$. We shall investigate the convergence behavior of the compensation algorithm in the following subsection.

B. Performance Analysis for the Compensation Algorithm

Suppose the functions $\hat{\varphi}_q(\mathbf{p}; \bullet)$ and $\hat{\varphi}_h(\mathbf{p}; \bullet)$ are Lipschitz continuous, i.e., there exists positive constants L_q, $L_h < \infty$, such that $\|\hat{\varphi}_q(\mathbf{p}; \bullet) - \hat{\varphi}_q(\mathbf{p}^*; \bullet)\| \leq L_q \|\mathbf{p} - \mathbf{p}^*\|$ and $\|\hat{\varphi}_h(\mathbf{p}; \bullet) - \hat{\varphi}_h(\mathbf{p}^*; \bullet)\| \leq L_h \|\mathbf{p} - \mathbf{p}^*\|$, for all $\mathbf{p} \in \mathbb{R}_+^L$. Let $\mu_{\max}$ be the maximum transmission rate that the system can support and $\alpha > 0$ be defined in (19) uniformly for all CSI realization $\mathbf{h}$. The following theorem provides a sufficient condition to the convergence of the compensation algorithm.

Theorem 4 (Convergence of the Compensation Algorithm): Provided that the step size parameter κ satisfies,

$$\kappa \;>\; \frac{1}{\alpha}\left[(\mu_{\max} + \lambda_{\max}L)\,L_q + \frac{1}{2}L_q^2 + \frac{1}{2}a_A L_h^2\right]$$

for all $t \geq 0$. Then the MWQ iterations with compensation in (29) asymptotically tracks the moving equilibrium point $\mathbf{p}^*(t)$ with no errors, i.e., $\forall \epsilon > 0$,

$$\lim_{t \to 0} \Pr\left[\|\mathbf{p}(t) - \mathbf{p}^*(t)\| < \epsilon\right] = 1.$$

∎

Proof: Please refer to Appendix G for the proof. ∎

Theorem 4 shows that when a large enough step size κ is available, the compensation algorithm can converge to the equilibrium point $\mathbf{p}^*(t)$, and there is no performance penalty due to the time-varying CSI and QSI. The convergence is affected by the parameters L, a_A, L_h and L_q, where L is number of transmission links in the network (the system dimension), a_A is the CSI variation rate of the whole network, and L_h and L_q represent the sensitivity of the equilibrium point $\mathbf{p}^*(t)$ w.r.t. the time-varying CSI and QSI. On the other hand, for conventional gradient iteration in (9), the algorithm cannot have $\mathbf{p}_e \to \mathbf{0}$ no matter how large the iteration step size κ is used. This is due to the fact that the target equilibrium $\mathbf{p}^*(t)$ is moving due to the time-varying CSI and QSI.

Remark 1 (Interpretation of the results): In practice, we would like to implement the modified MWQ iteration in (29) on discrete time. The iterations of (29) can be written as

$$\mathbf{p}(t + \tau) = \left\{\mathbf{p}(t) + \kappa\tau\nabla\mathcal{L}(\mathbf{p}(t); \mathbf{h}(t), \mathbf{q}(t)) - \hat{\varphi}_q(\bullet)\triangle\mathbf{q}(t) - \mathrm{Re}\left[\hat{\varphi}_h(\bullet)\triangle\mathbf{h}(t)\right]\right\}_{\mathbf{p}}^{\mathcal{P}}$$

in discrete time where $\triangle x(t) = x(t+\tau) - x(t)$ and τ is the time step. In this case, the overall error between $\mathbf{p}(t)$ and $\mathbf{p}^*(t)$ is contributed by (a) algorithm convergence error and (b) steady state error. While Theorem 4 suggests that a large step size κ is always desirable from the algorithm convergence error perspective, the above analysis did not consider the *steady state error* (due to constant step size) $o(\kappa\tau)$ associated with discrete-time implementation. The overall impacts of steady state errors and tracking errors will be demonstrated in the numerical results section.

V. NUMERICAL RESULTS AND DISCUSSIONS

In this section, we shall simulate the tracking performance of the conventional MWQ iteration and the proposed compensated MWQ iteration in time-varying channels. We also demonstrate the delay performance for the two MWQ iterations under various CSI fading rates. We consider a wireless ad-hoc network with 5 nodes and 6 links as depicted in Fig. 1. The l-th link transmits the l-th data flow. Transmission flows towards a same destination share the same frequency band and SIC is implemented at each receiving node to handle the inter-flow interference. The CSI h_l for each link is modeled by a unit variance Markov process described by the SDE in (2). Data arrivals are modeled by continuous time Poisson processes with rate $\lambda = 20$ packets/second. All the algorithms are implemented in discrete-time iterations with simulation time step 1 ms and the queueing system was run over a time duration $T = 100$ min. The delay performance of the conventional MWQ iterations in (9) and the modified MWQ iterations with compensation in (29) are compared against the following reference baselines.

- **Baseline 1 - Constant Power Allocation:** At each time slot, fixed power P is allocated to each link and the transmission rate is computed by (6)-(7).
- **Baseline 2 - Throughput Optimal Power Allocation:** The throughput optimal power control is computed by solving the MWQ problem in (4)-(5) to obtain the target equilibrium $\mathbf{p}^*(\mathbf{h}, \mathbf{q})$ at each time slot t.

A. Power Tracking Performance of the MWQ Iterations

Fig. 5 captures the power control algorithm trajectory $\mathbf{p}(t)$ versus time at a CSI fading rate of $a_A = 200$. The algorithms update on every $\tau = 1$ ms time slot and the step size is chosen to be 0.5 (corresponding to $\kappa = 500$ sec^{-1} for continuous-time trajectory). Throughout the simulation, the average delay is measured as $\overline{T}_l \approx 500$ ms. As illustrated, the target equilibrium $p_1^*(t)$ changes significantly over time due to the time varying CSI. The conventional MWQ iterations $p_{MWQ,1}(t)$ fail to track the moving target $p_1^*(t)$ accurately but the trajectory of the compensated MWQ iterations $p_{com,1}(t)$ can track the moving target quite well.
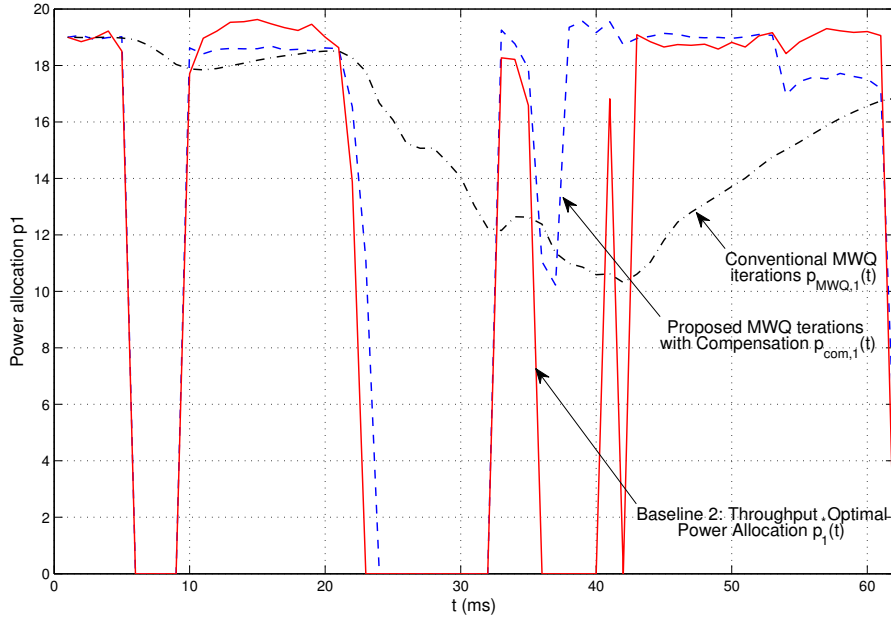
Figure 5. The power control algorithm trajectory $\mathbf{p}(t)$ versus time at a CSI fading rate a_A = 200 and packet arrival rate $\lambda = 20$ packets/second. The algorithms update on every $\tau = 1$ ms time slot with step size 0.5 (corresponding to $\kappa = 500$ sec^{-1}). The average delay is measured to be $\overline{T}_l \approx 500$ ms. As illustrated, the target equilibrium $p_1^*(t)$ changes significantly over time due to the time varying CSI. The conventional MWQ iterations $p_{MWQ,1}(t)$ fail to track the moving target $p_1^*(t)$ accurately but the trajectory of the compensated MWQ iterations $p_{com,1}(t)$ can track the moving target quite well.

Fig. 6 illustrates the average tracking error of the power trajectory $\mathbf{p}(t)$ versus the fading rate a_A. The average tracking error of the power trajectory is defined as $e = \frac{1}{T} \int_0^T \|\mathbf{p}(t) - \mathbf{p}^*(t)\| dt$. It is shown that the average tracking error of conventional MWQ iterations increases with the fading rate a_A. On the other hand, the tracking error of the modified MWQ iterations (with compensations) is much smaller[8] than that of the conventional MWQ iterations.

B. Power-Delay Tradeoff Performance

Fig. 7 illustrates the per-node average power versus the average delay at different fading rates. Note that along each curve, we have different values of V, which acts as a tradeoff parameter for power-delay tradeoff. Small V corresponds to small delay and vice versa. Observed that to maintain the same average delay of 2 seconds, the conventional MWQ iterations require 2.3 dB more power

---

[8]Note that the tracking error shown is the overall error obtained using discrete-time iterations, which include the errors due to algorithm convergence and *steady state errors* (due to constant discrete time step size). From Theorem 4, the algorithm convergence error tends to zero for the modified MWQ but there is a steady state error in Fig. 6 due to the constant step size in discrete time implementation.
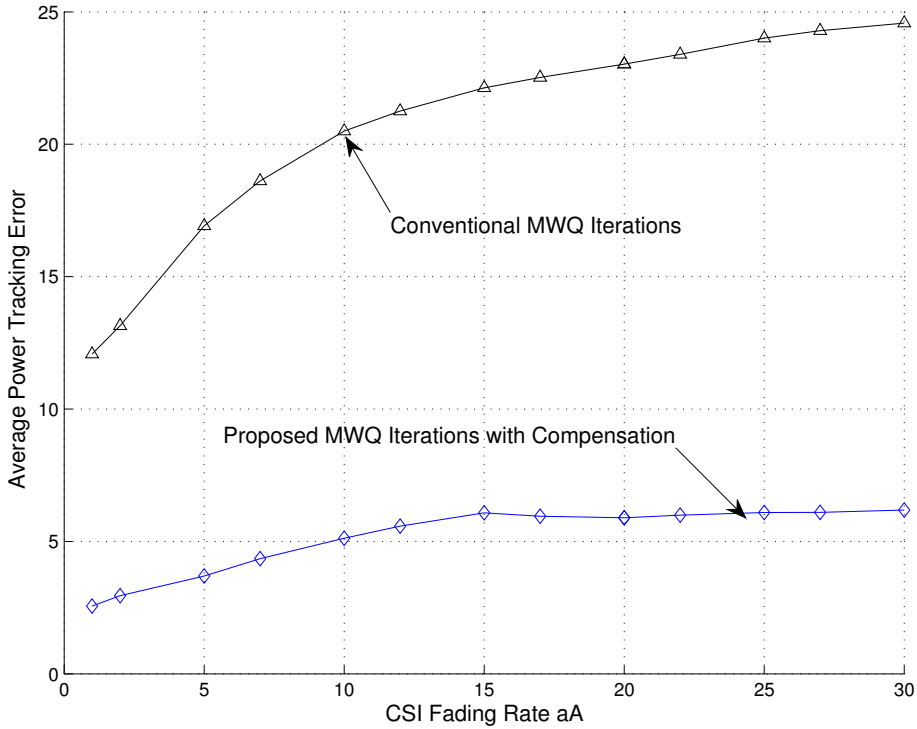
Figure 6. The average tracking error of the power trajectory $\mathbf{p}(t)$ versus the fading rate a_A under packet arrival rate $\lambda = 20$ packets/second. The algorithms update on every $\tau = 1$ ms time slot with step size 0.5 (corresponding to $\kappa = 500 \text{ sec}^{-1}$). The average tracking error of conventional MWQ iterations increases with the fading rate a_A. On the other hand, the tracking error of the modified MWQ iterations (with compensations) is much smaller than that of the conventional MWQ iterations. Note that the error consists of contributions from both the algorithm convergence error and steady state error due to constant step size (in discrete time). From Theorem 4, the algorithm convergence error of the modified MWQ converges to zero but there is still residual steady state error.

than the throughput optimal scheme. On the other hand, the proposed modified MWQ algorithm with compensation suffers from a very small power penalty (< 1dB) compared with baseline 2 (the throughput optimal scheme). Furthermore, as the CSI fading rate a_A increases, the conventional MWQ iterations eventually require as much power as baseline 1 (constant power allocation) does, while the proposed modified MWQ algorithm with compensation still has a reasonable power gain compared to baseline 1.

VI. Conclusions

In this paper, we have analyzed the convergence behavior and the queue delay performance of the conventional MWQ iterations in a wireless adhoc network, in which the CSI and the QSI are changing in a similar timescale as the algorithm iterations. We first show that the algorithm convergence can be captured by studying the stochastic stability of an equivalent *virtual stochastic dynamic system*
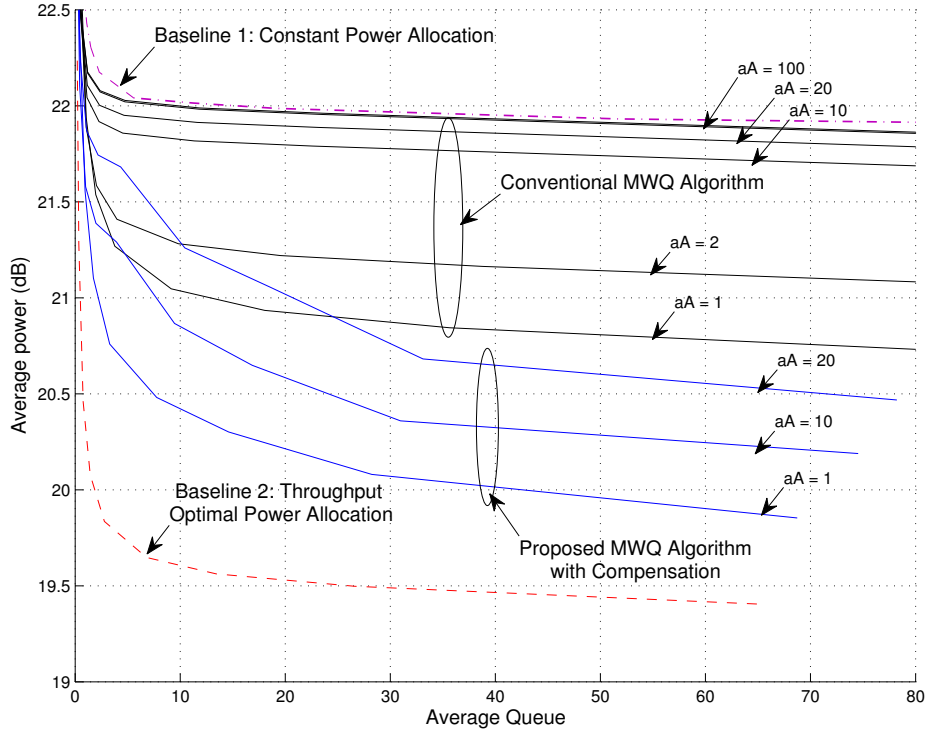
Figure 7. The per-node average power versus the average delay at different fading rate. Observed that to maintain the same average delay of 2 seconds, the conventional MWQ iterations require 2.3 dB more power than the throughput optimal scheme. On the other hand, the proposed modified MWQ algorithm with compensation suffers from a very small power penalty (< 1dB) compared with baseline 2 (the throughput optimal scheme). Furthermore, as the CSI fading rate a_A increases, the conventional MWQ iterations eventually require as much power as baseline 1 (constant power allocation) does, while the proposed modified MWQ algorithm with compensation still has a reasonable power gain compared to baseline 1.

(VSDS). By extending the Foster-Lyapunov criteria, we established the technical conditions for queue stability and derived the associated queue bounds. Based on these analyses, we have proposed a novel adaptive MWQ algorithm with a predictive compensation to counteract the effects of the time varying CSI and QSI. We have demonstrated that with some mild conditions, the modified MWQ iterations (with compensation) can converge to the moving target power $\mathbf{p}^*(t)$ despite the time varying CSI and QSI. Finally, simulation results demonstrated the performance gain of the proposed algorithm in both the network delay performance and the tracking error of the power trajectory.

APPENDIX A

CONNECTIONS BETWEEN THE OPTIMIZATION ALGORITHMS AND THE VSDS

In this section, we give a brief introduction to the Lyapunov method for algorithm convergence analysis, which motivates us to connect the algorithm trajectory to the VSDS.

We focus on gradient-based methods that are widely used for computing the optimal resource allocations in wireless communication networks and are well-suited for implementations across a distributed network. The gradient method searches the optimum point x^* of the objective function $\mathcal{L}(x)$ following

$$\dot{x} = \frac{dx}{dt} = \kappa \left[\frac{\partial \mathcal{L}}{\partial x}\right]^T.$$

Here we study the convergence behavior by constructing the tracking *error dynamics* of the algorithm trajectory. Define the tracking error $x_e = x - x^*$ and substitute it into the above dynamics, we obtain

$$\dot{x}_e = \kappa \left[\frac{\partial \mathcal{L}(x_e + x^*)}{\partial x_e}\right]^T \triangleq f(x_e). \tag{30}$$

Hence the convergence analysis is transferred to stability analysis [23] of the virtual error dynamic system (30) at the origin $x_e = 0$.

A classic method to study the stability of a dynamic system is via the Lyapunov theory [23]. We first construct a Lyapunov function which has the following properties,

$$V(x_e) \to \infty, \text{ as } \|x_e\| \to \infty, \quad \text{and } V(x_e) \to 0, \text{ as } \|x_e\| \to 0.$$

The Lyapunov theory says, if $\dot{V}(x_e) < 0$ for all $x_e \in \mathbb{R}^n \backslash \{0\}$, then the dynamic system $\dot{x}_e = f(x_e)$ is asymptotically stable at the origin $x_e = 0$ [23].

Note that, the objective function $\mathcal{L}(x; h(t), q(t))$ we focus on in this paper has stochastic time-varying parameters $h(t)$ and $q(t)$, which may evolve in a similar timescale to the algorithm trajectory. We tackle this problem by constructing the VSDS from the algorithm dynamics, and extending the Foster-Lyapunov criteria (in Theorem 2). We show the connection between the algorithm trajectory and the VSDS in the following.

Proof of Theorem 1: Note that the VSDS in (15) consists of three components, $\mathbf{p}_e$, $\mathbf{h}$ and $\mathbf{q}$, where the dynamics of $\mathbf{h}(t)$ and $\mathbf{q}(t)$ are just the same as (11) and (12). We only need to show that the dynamics of $\mathbf{p}_e(t)$ in the VSDS in (15) implies the MWQ power control algorithm dynamics of $\mathbf{p}(t)$ in (10). Equivalently, we need to show

$$\mathbf{p}(t) = \mathbf{p}_e(0) + \int_0^t d\mathbf{p}_e(\tau) + \mathbf{p}^*(t)$$

to be the solution of (10). On the other hand, by the definition of tracking error (Definition 3), $\mathbf{p}_e(0) + \int_0^t d\mathbf{p}_e(\tau) + \mathbf{p}^*(t) = \mathbf{p}_e(t) + \mathbf{p}^*(t) = \mathbf{p}(t)$. Therefore, by substituting $\mathbf{p}_e(t) + \mathbf{p}^*(t)$ with $\mathbf{p}(t)$ in the VSDS in (15), we see that the trajectory $\mathbf{q}(t)$ in the VSDS is just the same as that in (12).

To prove the second part of the theorem, we consider that there is no disturbance applied to the SEDS in (14) by considering $d\mathbf{N} \equiv \mathbf{0}$ and $d\mathbf{W} \equiv \mathbf{0}$. Equivalently, we take $d\mathbf{h} = \mathbf{0}$ and $d\mathbf{q} = \mathbf{0}$ in (13). The SDE of $\mathbf{p}_e(t)$ in (14) reduces to

$$d\mathbf{p}_e = \kappa \left[\nabla \mathcal{L}\left(\mathbf{p}_e + \mathbf{p}^*; \mathbf{h}, \mathbf{q}\right)\right]_{\mathbf{p}_e + \mathbf{p}^*}^+ dt. \tag{31}$$

By the definition of equilibrium point (Definition 2), $\mathbf{p}_e \to \mathbf{0}$ corresponds to $\nabla \mathcal{L} \to \mathbf{0}$. Hence the origin is an equilibrium to the SDE in (14). On the other hand, if the origin is an equilibrium to (31), $\mathbf{p}^* = \psi(\mathbf{h}, \mathbf{q})$ must be the equilibrium to the dynamics of the power control algorithm in (10). Hence, we complete the proof.

APPENDIX B

PROOF OF THEOREM 2

Proof: Define a sequence of stopping time $t_n = \inf \{t \geq 0 : \mathbf{z}(t) \geq n\}$. By Dynkin's formula [25],

$$0 \leq V(\mathbf{z}(t_n)) \leq V(\mathbf{z}(0)) + \mathbb{E}\left[\int_0^{t_n} (-a\|\mathbf{z}(\tau)\| + g(\mathbf{s}(\tau)))\, d\tau\right].$$

Hence we have

$$\mathbb{E}\left[\int_0^{t_n} a\|\mathbf{z}(\tau)\| d\tau\right] \leq V(\mathbf{z}(0)) + \mathbb{E}\left[\int_0^{t_n} g(\mathbf{s}(\tau)) d\tau\right]$$

Exchanging the order of integration and expectation, we have

$$\frac{1}{t_n} \int_0^{t_n} \mathbb{E}\|\mathbf{z}(\tau)\| d\tau \leq \frac{1}{t_n} \frac{V(\mathbf{z}(0))}{a} + \frac{1}{t_n} \int_0^{t_n} \mathbb{E}\left[g(\mathbf{s}(\tau))\right] d\tau$$

Taking limit on both sides, we obtain

$$\limsup_{n \to \infty} \frac{1}{t_n} \int_0^{t_n} \mathbb{E}\|\mathbf{z}(\tau)\| d\tau \leq \limsup_{n \to \infty} \left(\frac{1}{t_n} \frac{V(\mathbf{z}(0)}{a} + \frac{1}{t_n} \int_0^{t_n} \frac{1}{a} \mathbb{E}\left[g(\mathbf{s}(\tau))\right]\right) \leq \frac{d}{a}.$$

Notice that $t_n \to \infty$ as $n \to \infty$, and $V(\mathbf{z}(0))$ is bounded. Thus the result holds. $\blacksquare$

APPENDIX C

PROOF OF LEMMA 3

Proof: According to Lemma 1, the optimization problem (8) can be written as

$$\max_{\mathbf{p} \in \mathcal{P}} \quad q_{\pi(1)} \log \left(1 + |h_{\pi(1)}|^2 p_{\pi(1)}\right) \tag{32}$$

$$+ q_{\pi(2)} \left[\log \left(1 + \left|h_{\pi(1)}\right|^2 p_{\pi(1)} + \left|h_{\pi(2)}\right|^2 p_{\pi(2)}\right) - \log \left(1 + |h_{\pi(1)}|^2 p_{\pi(1)}\right)\right] + \ldots$$

$$+ q_{\pi(L)} \left[\log \left(1 + \sum_{i=1}^{L} \left|h_{\pi(i)}\right|^2 p_{\pi(i)}\right) - \log \left(1 + \sum_{i=1}^{L-1} \left|h_{\pi(i)}\right|^2 p_{\pi(i)}\right)\right] - \sum_{i=1}^{L} V p_{\pi(i)}$$

for a certain permutation $\boldsymbol{\pi}$, where $q_{\pi(k-1)} \geq q_{\pi(k)}$, for $k = 2, \ldots, L$. As the objective function $\mathcal{L}(\mathbf{p}; \mathbf{h}, \mathbf{q})$ is a combination of logarithmic functions, it can be verified that $\mathcal{L}(\mathbf{p}; \mathbf{h}, \mathbf{q})$ is strictly concave in $\mathbf{p}$ and $\nabla^2 \mathcal{L}(\mathbf{p}; \mathbf{h}, \mathbf{q}) < 0$. In addition, as the domain $\mathcal{P}$ is compact and under the condition that $q_{\pi(i)} \geq 1$, there exists a positive constant $\alpha(S_{\min}, S_{\max}) > 0$ depending only on the channel gain parameters $S_{\min}(t)$ and $S_{\max}(t)$, such that the Hessian of $\mathcal{L}(\mathbf{p}; \mathbf{h}, \mathbf{q})$ satisfies $\nabla^2 \mathcal{L} \preceq -\alpha \mathbf{I}$ for all $\mathbf{p} \in \mathcal{P}$.

Based on this observation, we obtain,

$$
\mathbf{p}_e^T f(\mathbf{p}_e; \mathbf{h}, \mathbf{q}) = \mathbf{p}_e^T f(\mathbf{0}_+; \mathbf{h}, \mathbf{q}) + \mathbf{p}_e^T \int_0^1 \nabla f(\xi \mathbf{p}_e; \mathbf{h}, \mathbf{q}) d\xi \mathbf{p}_e \tag{33}
$$

$$
= \mathbf{p}_e^T f(\mathbf{0}_+; \mathbf{h}, \mathbf{q}) + \mathbf{p}_e^T \int_0^1 \kappa \nabla^2 \mathcal{L}(\xi \mathbf{p}_e + \mathbf{p}^*(\mathbf{h}, \mathbf{q}); \mathbf{h}, \mathbf{q}) d\xi \mathbf{p}_e \tag{34}
$$

$$
\leq - \int_0^1 \alpha \kappa \|\mathbf{p}_e\|^2 d\xi \tag{35}
$$

$$
= -\alpha \kappa \|\mathbf{p}_e\|^2
$$

where $\mathbf{p}_e^T f(\mathbf{0}_+; \mathbf{h}, \mathbf{q}) = (\mathbf{p} - \mathbf{p}^*)^T \nabla \mathcal{L}(\mathbf{p}^*(\mathbf{h}, \mathbf{q}); \mathbf{h}, \mathbf{q}) \leq 0$ is the optimality condition for $\mathbf{p}^*(\mathbf{h}, \mathbf{q})$ in the optimization problem (8). The equality (33) is from Taylor expansion of the gradient iteration function $f(.)$, the second equality (34) is from the fact that $\nabla f = \nabla^2 \mathcal{L}$, since $f = \nabla \mathcal{L}$, and the inequality (35) is from $\nabla^2 \mathcal{L} \preceq -\alpha \mathbf{I}$ derived above. Hence we proved the result. ∎

APPENDIX D

PROOF OF LEMMA 4

Proof: We first consider a time division MWQ policy. At each time slot, only the link is selected for transmission and the policy is given in the following [6].

1) Find a link $\hat{l}$ such that

$$
\hat{l} = \arg \max_{l=1,\ldots,L} \left\{ q_l \log(1 + |h_l|^2 p_l) - V p_l \right\} \tag{36}
$$

2) *Power allocation:* the power $\mathbf{p}$ is allocated according to

$$
\widetilde{p}_l =
\begin{cases}
\left(\frac{q_l}{V} - \frac{1}{|h_l|^2} \right)_{\widetilde{p}_l}^{\mathcal{P}} & l = \hat{l} \\
0 & \text{otherwise}
\end{cases} \tag{37}
$$

where the projection yields $\widetilde{p}_{\hat{l}} = \max\{0, \min\{q_l/V - 1/|h_l|^2, 2^{L\lambda_{\max}}/h_0^2\}\}$.

3) *Rate allocation:* the rate $\boldsymbol{\mu}$ is allocated according to

$$
\widetilde{\mu}_l =
\begin{cases}
\log \left(1 + \left(\frac{q_l |h_l|^2}{V} - 1 \right)_{\widetilde{p}_l}^{\mathcal{P}} \right) & l = \hat{l} \\
0 & \text{otherwise}
\end{cases} \tag{38}
$$

Note that the above policy is the solution of the following optimization problem,

$$
\text{maximize} \qquad \sum q_l \log(1 + |h_l|^2 p_l) - V \sum p_l \tag{39}
$$

$$
\text{subject to} \qquad \text{only one link is activated.}
$$

As a result, the optimum queue-weighted sum transmission rate for the time division policy is

$$
\begin{aligned}
\sum_{l=1}^{L} q_l \widetilde{\mu}_l &= q_{\hat{l}} \log\left(1 + \left(\frac{q_{\hat{l}}|h_{\hat{l}}|^2}{V} - 1\right)_{\widetilde{p}_{\hat{l}}}^{\mathcal{P}}\right) \geq q_m \log\left(1 + \left(\frac{q_m|h_m|^2}{V} - 1\right)_{p_m}^{\mathcal{P}}\right) \\
&= \begin{cases} 0 & \|\mathbf{q}\||h_m|^2 \leq V \\ q_m \min\left\{\log\left(\frac{|h_m|^2}{V} q_m\right), L\lambda_{\max} + \log\frac{|h_m|^2}{|h_0|^2}\right\} & \|\mathbf{q}\||h_m|^2 > V \end{cases} \\
&\geq \begin{cases} 0 & \|\mathbf{q}\|S_{\min} \leq V \\ \|\mathbf{q}\| \min\left\{\log\left(\frac{S_{\min}}{V}\|\mathbf{q}\|\right), L\lambda_{\max} + \log\frac{S_{\min}}{|h_0|^2}\right\} & \|\mathbf{q}\|S_{\min} > V \end{cases}
\end{aligned}
\tag{40}
$$

where $q_m = \|\mathbf{q}\|$ stands for the queue that has the largest backlog (i.e., $m = \arg\max_l\{q_l\}$). The optimal utility for the time division policy is then given by (40) for $\|\mathbf{q}\|S_{\min} > V$ where $P_t = \sum \widetilde{p}_l = p_{\hat{l}}$ is the total power.

Since, with the same objective, the optimization domain of the time division MWQ problem (39) is just a subset of that of the original MWQ problem in (4), the MWQ problem (4) yields a utility $U^* = \sum q_l \mu_l^* - V \sum p_l^* \geq \widetilde{U}$. To evaluate the queue-weighted utility $\sum q_l \mu_l^*$, we consider the following two cases.

Case 1: When $\sum p_l^* \geq P_t = \sum \widetilde{p}_l$, it is obvious that, for $\|\mathbf{q}\|S_{\min} > V$,

$$
\sum q_l \mu_l^* \geq \sum q_l \widetilde{\mu}_l \geq \|\mathbf{q}\| \min\left\{\log\left(\frac{S_{\min}}{V}\|\mathbf{q}\|\right), L\lambda_{\max} + \log\frac{S_{\min}}{|h_0|^2}\right\}.
$$

Case 2: When $\sum p_l^* < P_t$, we let $V' = \frac{\sum p_l^*}{P_t} V < V$. Note that decreasing the tradeoff parameter V will increase the power allocation and hence increase the queue-weighted utility $\sum q_l \mu_l^*$. Specifically, the optimal utility becomes

$$
U^* = \sum q_l \mu_l^* - V \sum p_l^* = \sum q_l \mu_l^* - V' P_t \geq \sum q_l \widetilde{\mu}_l' - V' P_t \geq \sum q_l \widetilde{\mu}_l' - V' \sum \widetilde{p}_l
$$

as

$$
\widetilde{p}_l = \begin{cases} \left(\frac{q_l}{V'} - \frac{1}{|h_l|^2}\right)_{\widetilde{p}_l}^{\mathcal{P}} \geq \widetilde{p}_l = P_t & l = \hat{l} \\ 0 & \text{otherwise} \end{cases}
$$

where $\widetilde{\mu}_l'$ and $\widetilde{p}_l$ are the solutions to the time division MWQ problem (39). Hence $\sum q_l \mu_l^* \geq \sum q_l \widetilde{\mu}_l' \geq \|\mathbf{q}\| \log\left(\frac{S_{\min}}{V'}\|\mathbf{q}\|\right) \geq \|\mathbf{q}\| \min\left\{\log\left(\frac{S_{\min}}{V}\|\mathbf{q}\|\right), L\lambda_{\max} + \log\frac{S_{\min}}{|h_0|^2}\right\}$, for $\|\mathbf{q}\|S_{\min} > V$.

Combining the above two cases, we prove the inequality (20).

In addition, as $L\|\mathbf{q}\|\|\boldsymbol{\mu}^*\| \geq \sum_{l=1}^{L} q_l \mu_l^* \geq \|\mathbf{q}\| \min\left\{\log\left(\frac{S_{\min}}{V}\|\mathbf{q}\|\right), L\lambda_{\max} + \log\frac{S_{\min}}{|h_0|^2}\right\}$, we have $\|\boldsymbol{\mu}^*\| \geq \frac{1}{L} \min\left\{\log\left(\frac{S_{\min}}{V}\|\mathbf{q}\|\right), L\lambda_{\max} + \log\frac{S_{\min}}{|h_0|^2}\right\}$, for $\|\mathbf{q}\|S_{\min} > V$. Similarly, we can get $\|\boldsymbol{\mu}^*\| \leq \log\left(\frac{S_{\max}}{V}\|\mathbf{q}\|\right)$. Hence we prove inequality (21). ∎

APPENDIX E

PROOF OF LEMMA 5

Proof: According to (7) in Lemma 1, $\hat{\mu}_{\pi(k)} = \log\left(\rho_k(\mathbf{p})\right)$ under some permutation $\boldsymbol{\pi}$, where

$$\rho_k(\mathbf{p}) = \frac{1 + \sum_{i=1}^{k} \left|h_{\pi(i)}\right|^2 p_{\pi(i)}}{1 + \sum_{i=1}^{k-1} \left|h_{\pi(i)}\right|^2 p_{\pi(i)}}.$$

Notice that $\rho_k(\mathbf{p})$ is a ratio of two polynomials. In addition, the coefficients $\left|h_{\pi(i)}\right|^2$ are bounded by $S_{\min}$ and $S_{\max}$. Hence $\rho_k(\mathbf{p})$ is Lipschitz continuous, i.e., there exists $0 < \beta_k < \infty$ depending on $S_{\min}$ and $S_{\max}$ such that

$$\|\rho_k(\mathbf{p}) - \rho(\mathbf{p}^*)\| \leq \beta_k \|\mathbf{p} - \mathbf{p}^*\| = \beta_k \|\mathbf{p}_e\|.$$

Therefore, as $\rho_k(.) \geq 1$, assuming $\rho_k(\mathbf{p}) \geq \rho(\mathbf{p}^*)$, we have

$$
\begin{aligned}
\|\hat{\mu}_{\pi(k)}(\mathbf{p}) - \hat{\mu}_{\pi(k)}(\mathbf{p}^*)\| &= \log\left(\rho_k(\mathbf{p})\right) - \log\left(\rho_k(\mathbf{p}^*)\right) \\
&= \log\left(1 + \frac{\rho_k(\mathbf{p}) - \rho_k(\mathbf{p}^*)}{\rho_k(\mathbf{p}^*)}\right) \leq \log\left(1 + \frac{\beta_k \|\mathbf{p}_e\|}{\rho_k(\mathbf{p}^*)}\right) \leq \log\left(1 + \beta_k \|\mathbf{p}_e\|\right).
\end{aligned}
$$

Similarly, when $\rho_k(\mathbf{p}) < \rho(\mathbf{p}^*)$, we have

$$
\begin{aligned}
\|\hat{\mu}_{\pi(k)}(\mathbf{p}) - \hat{\mu}_{\pi(k)}(\mathbf{p}^*)\| &= \log\left(\rho_k(\mathbf{p}^*)\right) - \log\left(\rho_k(\mathbf{p})\right) \\
&= \log\left(1 + \frac{\rho_k(\mathbf{p}^*) - \rho_k(\mathbf{p})}{\rho_k(\mathbf{p})}\right) \leq \log\left(1 + \frac{\beta_k \|\mathbf{p}_e\|}{\rho_k(\mathbf{p})}\right) \leq \log\left(1 + \beta_k \|\mathbf{p}_e\|\right).
\end{aligned}
$$

Hence $\|\hat{\boldsymbol{\mu}}(\mathbf{p}) - \hat{\boldsymbol{\mu}}(\mathbf{p}^*)\| \leq \log\left(1 + \beta \|\mathbf{p}_e\|\right)$, where $\beta = \max_{k=\{1,...,L\}} \beta_k$. Using the triangular inequality, we obtain

$$\|\hat{\boldsymbol{\mu}}(\mathbf{p}^*)\| - \log\left(1 + \beta \|\mathbf{p}_e\|\right) \leq \|\hat{\boldsymbol{\mu}}(\mathbf{p})\| \leq \|\hat{\boldsymbol{\mu}}(\mathbf{p}^*)\| + \log\left(1 + \beta \|\mathbf{p}_e\|\right)$$

that leads to the result. ∎

APPENDIX F

PROOF OF LEMMA 6

Proof: From Lemma 1 and 5, we have

$$
\begin{aligned}
\sum q_l \hat{\mu}_l(t) &\geq \sum q_l \left[\mu_l^* - \log\left(1 + \beta \|\mathbf{p}_e\|\right)\right]^+ \\
&\geq \sum q_l \mu_l^* - \sum q_l \log\left(1 + \beta \|\mathbf{p}_e\|\right) \\
&\geq \|\mathbf{q}\| \min\left\{\log\left(\frac{S_{\min}}{V} \|\mathbf{q}\|\right), L\lambda_{\max} + \log\frac{S_{\min}}{|h_0|^2}\right\} - L\|\mathbf{q}\| \log\left(1 + \beta \|\mathbf{p}_e\|\right)
\end{aligned}
$$

From the optimality condition [26] for a convex problem, we also have $\mathbf{p}_e^T f(\mathbf{p}_e; \mathbf{h}, \mathbf{q}) \leq 0$ for all $\mathbf{p}_e$. According to the proof of Lemma 4 in Appendix D, two cases for $\mathbf{q}(t)$ should be considered.

Case 1: $\|\mathbf{q}\|S_{\min} > V$. The stochastic Lyapunov drift (18) can be written as

$$
\begin{aligned}
LV(\mathbf{z}) \leq & -2\kappa\alpha\|\mathbf{p}_e\|^2 + 2\gamma_q\|\mathbf{p}_e\|\log\left(\frac{S_{\max}}{V}\|\mathbf{q}\|\right) + 2\gamma_q\|\mathbf{p}_e\|\log\left(1+\beta\|\mathbf{p}_e\|\right) \\
& +\gamma_h a_A\|\mathbf{p}_e\|\|\mathbf{h}\| - a_A\|\mathbf{h}\|^2 + 2\gamma_q\lambda_{\max}\|\mathbf{p}_e\| + 2L\|\mathbf{q}\|\log\left(1+\beta\|\mathbf{p}_e\|\right) \\
& -2\|\mathbf{q}\|\min\left\{\log\left(\frac{S_{\min}}{V}\|\mathbf{q}\|\right), L\lambda_{\max} + \log\frac{S_{\min}}{|h_0|^2}\right\} + 2L\|\mathbf{q}\|\lambda_{\max} + C \quad (41)
\end{aligned}
$$

where

$$
\begin{aligned}
\mathrm{tr}\left(2\left(A^{\frac{1}{2}}\right)^T \psi_h^T\psi_h A^{\frac{1}{2}} + \psi_q^T\psi_q\right) + \sum_{l=1}^{L}\left(2a_l+\lambda_l\right) & \leq \sum_{l=1}^{L} 2a_l\left(1+\gamma_h^2\right) + L\gamma_q^2 + \sum_{l=1}^{L}\lambda_l \\
& \leq L(2a_A(1+\gamma_h^2)+\gamma_q^2+\lambda_{\max}) \\
& \triangleq C
\end{aligned}
$$

To find the upper bound of the R.H.S. of (41), we divide it into 2 parts as follows.

$$
\begin{aligned}
I_1 = & -\kappa\alpha\|\mathbf{p}_e\|^2 + 2\gamma_q\lambda_{\max}\|\mathbf{p}_e\| - \|\mathbf{q}\|\min\left\{\log\left(\frac{S_{\min}}{V}\|\mathbf{q}\|\right), L\lambda_{\max} + \log\frac{S_{\min}}{|h_0|^2}\right\} \\
& +L\lambda_{\max}\|\mathbf{q}\| + 2\gamma_h a_A\|\mathbf{p}_e\|\|\mathbf{h}\| - 2a_A\|\mathbf{h}\|^2 + C, \\
I_2 = & -\kappa\alpha\|\mathbf{p}_e\|^2 + 2\gamma_q\|\mathbf{p}_e\|\log\left(\frac{S_{\max}}{V}\|\mathbf{q}\|\right) + 2\gamma_q\|\mathbf{p}_e\|\log\left(1+\beta\|\mathbf{p}_e\|\right) + L\lambda_{\max}\|\mathbf{q}\| \\
& +2L\|\mathbf{q}\|\log\left(1+\beta\|\mathbf{p}_e\|\right) - \|\mathbf{q}\|\min\left\{\log\left(\frac{S_{\min}}{V}\|\mathbf{q}\|\right), L\lambda_{\max} + \log\frac{S_{\min}}{|h_0|^2}\right\}.
\end{aligned}
$$

(1) With some calculations, it is not difficult to show that $I_1 \leq -\|\mathbf{h}\| + \frac{\gamma_q^2\lambda_{\max}^2}{\kappa\alpha} + \frac{V}{S_{\min}}2^{L\lambda_{\max}-1} + \frac{1}{8a_A[1-\gamma_h^2 a_A/(k\alpha)]} + C$, for $\kappa > \frac{2}{\alpha}\max\left\{\gamma_q^2, \beta\gamma_q\right\}$.

(2) Denote $g_1(S_{\min}, S_{\max}) = \max_{\{\|\mathbf{p}_e\|,\|\mathbf{q}\|\}}\left\{I_2 + (\|\mathbf{p}_e\| + \|\mathbf{q}\|)\right\}$. We can easily find that g_1 is bounded above for all $S_{\min}$ and $S_{\max}$ in the domain[9]. Note that an upper bound expression for g_1 is always obtainable, since it is only a simple bivariate programming problem. Therefore, we obtain $I_2 \leq -(\|\mathbf{p}_e\| + \|\mathbf{q}\|) + g_1(S_{\min}, S_{\max})$.

As a result, we have

$$
\begin{aligned}
LV \leq & -(\|\mathbf{p}_e\| + \|\mathbf{q}\| + \|\mathbf{h}\|) + \frac{\gamma_q^2\lambda_{\max}^2}{\kappa\alpha} + \frac{V}{S_{\min}}2^{L\lambda_{\max}-1} \\
& +\frac{1}{8a_A[1-\gamma_h^2 a_A/(k\alpha)]} + g_1(S_{\min}, S_{\max}) + C.
\end{aligned}
$$

Case 2: $\|\mathbf{q}\|S_{\min} \leq V$. Here we have $\|\mathbf{q}\| \leq \frac{V}{S_{\min}}$. From the property in Appendix D, the stochastic

---

[9]To show a real valued function $f(x,y)$ is bounded above, we start from a point (x_0, y_0) in the domain and proceed to show that, by substituting with $y = x_0 + \beta(y - y_0)$, $f(x, y(x;\beta))$ is bounded above uniformly for every $\beta \in \mathbb{R}$. It can be verified that $f(x, y(x;\beta))$ satisfies this condition in our case.

Lyapunov drift (18) can be written as

$$
\begin{aligned}
LV(\mathbf{z}) \leq\ & -2\kappa\alpha\|\mathbf{p}_e\|^2 + 2\gamma_q\|\mathbf{p}_e\|\log\left(S_{\max}S_{\min}\right) + 2\gamma_q\|\mathbf{p}_e\|\log\left(1+\beta\|\mathbf{p}_e\|\right) + \gamma_h a_A\|\mathbf{p}_e\|\|\mathbf{h}\| \\
& + 2\gamma_q\lambda_{\max}\|\mathbf{p}_e\| - a_A\|\mathbf{h}\|^2 + \frac{V}{S_{\min}}\log\left(1+\beta\|\mathbf{p}_e\|\right) + \frac{V}{S_{\min}}L\lambda_{\max} + C \\
\leq\ & -\left(\|\mathbf{p}_e\| + \|\mathbf{h}\|\right) + g_2(S_{\min},S_{\max}) + \frac{\gamma_q^2\lambda_{\max}^2}{\kappa\alpha} \\
& + \frac{V}{S_{\min}}L\lambda_{\max} + \frac{1}{8a_A[1-\gamma_h^2 a_A/(k\alpha)]} + C \\
\leq\ & -\left(\|\mathbf{p}_e\| + \|\mathbf{h}\|\right) + J_0 + \frac{\gamma_q^2\lambda_{\max}^2}{\kappa\alpha} + \frac{V}{S_{\min}}L\lambda_{\max} \\
& + \frac{1}{8a_A[1-\gamma_h^2 a_A/(k\alpha)]} + C - \|\mathbf{q}\| + \frac{V}{S_{\min}}
\end{aligned}
$$

where

$$
\begin{aligned}
g_2(S_{\min},S_{\max}) =\ & \max\{-\kappa\alpha\|\mathbf{p}_e\|^2 + 2\gamma_q\|\mathbf{p}_e\|\log\left(S_{\max}S_{\min}\right) \\
& + 2\gamma_q\|\mathbf{p}_e\|\log\left(1+\beta\|\mathbf{p}_e\|\right) + \frac{V}{S_{\min}}\log\left(1+\beta\|\mathbf{p}_e\|\right)\}.
\end{aligned}
$$

Therefore, we have [since $C = L(2a_A(1+\gamma_h^2) + \gamma_q^2 + \lambda_{\max})$]

$$
\begin{aligned}
LV(\mathbf{z}) \leq\ & -\left(\|\mathbf{p}_e\| + \|\mathbf{q}\| + \|\mathbf{h}\|\right) + L(2a_A(1+\gamma_h^2) + \gamma_q^2 + \lambda_{\max}) \\
& + \frac{\gamma_q^2\lambda_{\max}^2}{\kappa\alpha} + \frac{V}{S_{\min}}2^{L\lambda_{\max}-1} + \frac{1}{8a_A[1-\gamma_h^2 a_A/(k\alpha)]} + g(S_{\min},S_{\max})
\end{aligned}
$$

where $g(S_{\min},S_{\max}) = \max\left\{g_1(S_{\min},S_{\max}), g_1(S_{\min},S_{\max})\right\}$. ∎

APPENDIX G

PROOF OF THEOREM 4

Proof: Consider the virtual error dynamic system

$$
\begin{aligned}
d\mathbf{p}_e =\ & \kappa\nabla_{\mathbf{p}}\mathcal{L}\left(\hat{\boldsymbol{\mu}}(\mathbf{p}),\mathbf{p};\mathbf{h},\mathbf{q}\right)dt + \left(\hat{\varphi}_q(\mathbf{p};\bullet) - \hat{\varphi}_q(\mathbf{p}^*;\bullet)\right)d\mathbf{q} + \mathrm{Re}\left(\hat{\varphi}_h(\mathbf{p};\bullet)d\mathbf{h} - \hat{\varphi}_h(\mathbf{p}^*;\bullet)d\mathbf{h}\right) \\
=\ & \left[\kappa\nabla_{\mathbf{p}}\mathcal{L}\left(\hat{\boldsymbol{\mu}}(\mathbf{p}),\mathbf{p};\mathbf{h},\mathbf{q}\right) - \boldsymbol{\mu}(t)\left(\hat{\varphi}_q(\mathbf{p};\bullet) - \hat{\varphi}_q(\mathbf{p}^*;\bullet)\right) - \frac{1}{2}\mathrm{Re}\left[\left(\hat{\varphi}_h(\mathbf{p};\bullet) - \hat{\varphi}_h(\mathbf{p}^*;\bullet)\right)A\mathbf{h}\right]\right]dt \\
& + \left(\hat{\varphi}_q(\mathbf{p};\bullet) - \hat{\varphi}_q(\mathbf{p}^*;\bullet)\right)d\mathbf{N}(t) + \mathrm{Re}\left[\left(\hat{\varphi}_h(\mathbf{p};\bullet) - \hat{\varphi}_h(\mathbf{p}^*;\bullet)\right)A^{\frac{1}{2}}d\mathbf{W}(t)\right].
\end{aligned}
$$

Taking the Lyapunov function as $V(\mathbf{p}_e) = \frac{1}{2}\mathbf{p}_e^T \mathbf{p}_e$. The Lyapunov drift is defined as $LV(\mathbf{p}_e) = \lim_{\delta \downarrow 0} \frac{1}{\delta} \{\mathbb{E}\left[V\left(\mathbf{p}_e(t+\delta)\right)|\mathbf{p}_e(t)\right] - V\left(\mathbf{p}_e(t)\right)\}$. Note that $\mathbb{E}\left[h_l\right] = 0$. The drift can be derived into

$$
\begin{aligned}
LV(\mathbf{p}_e) &= \mathbf{p}_e^T f(\mathbf{p}_e; \cdot) - \mathbf{p}_e^T \boldsymbol{\mu}(t) \left(\hat{\varphi}_q(\mathbf{p}; \cdot) - \hat{\varphi}_q(\mathbf{p}^*; \cdot)\right) + \sum_{l=1}^{L} \lambda_l \mathbf{p}_e^T \left(\hat{\varphi}_q^{(l)}(\mathbf{p}; \cdot) - \hat{\varphi}_q^{(l)}(\mathbf{p}^*; \cdot)\right) \\
&\quad + \frac{1}{2}\text{tr}\left[\left(\hat{\varphi}_q(\mathbf{p}; \cdot) - \hat{\varphi}_q(\mathbf{p}^*; \cdot)\right)^T \left(\hat{\varphi}_q(\mathbf{p}; \cdot) - \hat{\varphi}_q(\mathbf{p}^*; \cdot)\right)\right] \\
&\quad + \frac{1}{2}\text{tr}\left[\left(A^{\frac{1}{2}}\right)^T \left(\hat{\varphi}_h(\mathbf{p}; \cdot) - \hat{\varphi}_h(\mathbf{p}^*; \cdot)\right)^T \left(\hat{\varphi}_h(\mathbf{p}; \cdot) - \hat{\varphi}_h(\mathbf{p}^*; \cdot)\right) A^{\frac{1}{2}}\right] \\
&\leq -\kappa\alpha\|\mathbf{p}_e\|^2 + \mu_{\max}L_q\|\mathbf{p}_e\|^2 + \lambda_{\max}LL_q\|\mathbf{p}_e\|^2 + \frac{1}{2}L_q^2\|\mathbf{p}_e\|^2 + \frac{1}{2}a_A L_h^2\|\mathbf{p}_e\|^2 \\
&= -\rho\|\mathbf{p}_e\|^2
\end{aligned}
$$

where $\rho = -\kappa\alpha + \mu_{\max}L_q + \lambda_{\max}LL_q + \frac{1}{2}L_q^2 + \frac{1}{2}a_A L_h^2 > 0$. Hence from the asymptotic stochastic stability results given in [25] we have proven the theorem. ∎

REFERENCES

[1] R. Berry and R. Gallager, "Communication over fading channels with delay constraints," *IEEE Transactions on Information Theory*, vol. 48, no. 5, pp. 1135 –1149, May 2002.

[2] I. Bettesh and S. Shamai, "Optimal power and rate control for minimal average delay: The single-user case," *IEEE Transactions on Information Theory*, vol. 52, no. 9, pp. 4115 –4141, Sept 2006.

[3] M. Goyal, A. Kumar, and V. Sharma, "Power constrained and delay optimal policies for scheduling transmission over a fading channel," in *IEEE INFOCOM 2003*, vol. 1, march-3 april 2003, pp. 311 – 320 vol.1.

[4] W. Wu, A. Arapostathis, and S. Shakkottai, "Optimal power allocation for a time-varying wireless channel under heavy-traffic approximation," *IEEE Transactions on Automatic Control*, vol. 51, no. 4, pp. 580 – 594, Apr 2006.

[5] L. Georgiadis, M. J. Neely, and L. Tassiulas, "Resource allocation and cross-layer control in wireless networks," *Now Publishers*, vol. 1, pp. 1–144, April 2006. [Online]. Available: http://portal.acm.org/citation.cfm?id=1166401.1166402

[6] M. Neely, "Energy optimal control for time-varying wireless networks," *IEEE Transactions on Information Theory*, vol. 52, no. 7, pp. 2915 –2934, July 2006.

[7] T. Holliday, A. Goldsmith, N. Bambos, and P. Glynn, "Distributed power and admission control for time-varying wireless networks," in *International Symposium on Information Theory, ISIT 2004*, 2004, p. 352.

[8] A. Paul, M. Akar, U. Mitra, and M. Safonov, "A switched system model for stability analysis of distributed power control algorithms for cellular communications," in *Proceedings of American Control Conference, 2004*, vol. 2, 30 2004-july 2 2004, pp. 1655 –1660 vol.2.

[9] R. Karthik and J. Kuri, "Convergence of power control in a random channel environment," in *IEEE Global Telecommunications Conference, GLOBECOM 2008*, Dec 2008, pp. 1 –5.

[10] V. Kavitha and V. Sharma, "Tracking analysis of an LMS decision feedback equalizer for a wireless channel," in *13th European Wireless Conference*, Paris, France, April 2007.

[11] G.M.Buckstein, "Distributed adaptive estimation and tracking using ad hoc wireless sensor networks," Ph.D. dissertation, Univ. of Minnesota, July 2009.

[12] J. Chen, V. Lau, and Y. Cheng, "Distributive network utility maximization over time-varying fading channels," *IEEE Transactions on Signal Processing*, vol. 59, no. 5, pp. 2395 –2404, may 2011.

[13] D. Tse and P. Viswanath, *Fundamentals of Wireless Communication*. Cambridge University Press, 2005.

[14] A. V. Skorohod, "Stochastic equations for di§usion processes in a bounded region," *Theory of Probability and Its Applications*, vol. 6, pp. 264–274, 1961.

[15] T. S. Feng, T. R. Field, and S. Haykin, "Stochastic Differential Equation Theory Applied to Wireless Channels," *IEEE Transactions on Communications*, vol. 55, no. 8, pp. 1478–1483, Aug. 2007.

[16] J. D. C. Little, "A proof for the queuing formula: L= λ w," *Operations Research*, vol. 9, no. 3, pp. 383–387, May 1961.

[17] L. Tassiulas and a. Ephremides, "Stability properties of constrained queueing systems and scheduling policies for maximum throughput in multihop radio networks," *IEEE Transactions on Automatic Control*, vol. 37, no. 12, pp. 1936–1948, 1992.

[18] D. Tse and S. Hanly, "Multiaccess fading channels I. Polymatroid structure, optimal resource allocation and throughput capacities," *IEEE Transactions on Information Theory*, vol. 44, no. 7, pp. 2796–2815, 1998.

[19] K. J. Arrow, L. Hurwicz, and H. Uzawa, *Studies in linear and non-linear programming*. California, Stanford: Stanford University Press, 1958.

[20] D. Feijer and F. Paganini, "Stability of primal-dual gradient dynamics and applications to network optimization," *Automatica*, vol. 46, pp. 1974–1981, Dec 2010. [Online]. Available: http://dx.doi.org/10.1016/j.automatica.2010.08.011

[21] D. Brandwood, "A complex gradient operator and its application in adaptive array theory," *IEE Proceedings H Microwaves, Optics and Antennas*, vol. 130, no. 1, p. 11, 1983.

[22] S. P. Meyn and R. L. Tweedie, "Stability of markovian processes III: Foster-Lyapunov criteria for continuous-time processes," *Advances in Applied Probability*, vol. 25, no. 3, pp. 518–548, Sept 1993.

[23] H. K. Khalil, *Nonlinear Systems*. Prentice-Hall, 1996.

[24] H. J. Kushner, *Stochastic stability and control*. Academic Press, New York, 1967.

[25] X. Mao, *Stochastic differential equations and their applications*. Horwood Pub., 1997.

[26] S. Boyd and L. Vandenberghe, *Convex Optimization*. Cambridge University Press, 2004.